Cavity ring-down spectrometers as monitoring tools: calibration, interference, and field-based isotopic measurements of CO_2 on Turrialba volcano, Costa Rica

by

Kalina Sophia Malowany

A THESIS

SUBMITTED TO MCGILL UNIVERSITY

IN PARTIAL FULFILMENT OF THE REQUIREMENTS FOR THE

DEGREE OF MASTERS OF SCIENCE

DEPARTMENT OF EARTH AND PLANETARY SCIENCES

MCGILL UNIVERSITY

MONTREAL, QUEBEC

JULY, 2015

Abstract

Carbon isotopic studies are valuable for understanding the degassing behaviour of an active volcano. The isotopic signature of CO_2 retains information regarding the magma composition and its degassing history. Newly available portable cavity ring-down spectrometers (CRDS) capable of making real-time isotopic measurements are changing the way in which isotope studies are being conducted, allowing for monitoring of isotopic CO_2 without the preparation and analysis time required for traditional mass spectrometry. Cavity ring-down spectrometers were originally developed as atmospheric instruments and are now being exploited as tools for monitoring of volcanic gases. These instruments were not initially tested in hot and acidic environments similar to those at active volcanoes; in some cases interference with the CRDS arise in these extreme environments. Laboratory experiments reveal that hydrogen sulfide gas has a significant spectral interference with the ^{12}C and ^{13}C spectral lines of the CRDS leading to erroneous $\delta^{13}C$ measurements with H_2S concentrations in excess of 10 ppb. To use these instruments on volcanoes, where H_2S concentrations can exceed 20 ppm, a copper metal scrub can be employed to remove all H_2S from gas samples without affecting the $\delta^{13}C$ value of the CO_2 gas. Furthermore, by combining CRDS carbon isotopic measurements taken in near real-time with standard isotopic measurements by isotope ratio mass spectrometry, we observe that the CRDS reports $\delta^{13}C$ values which are within error of traditional isotope ratio mass spectrometry (IRMS). Complementary measurements with the CRDS and IRMS were made on Turrialba volcano, Costa Rica, to characterize the isotopic signature of an increasingly active volcano and illustrate the application of CRDS for isotopic surveys of volcanoes. The isotopic composition of CO_2 from soil gases, the volcanic plume and high temperature vents reveals heterogeneity in the isotopic signature at Turrialba. Modification of the magmatic signature is

thought to result from interaction with a shallow hydrothermal system that buffers $\delta^{13}C$ to more enriched values. The high temperature vent gases preserve an unaltered isotopic signature consistent with a partially degassed magma below Turrialba. Isotopic plume measurements using the CRDS were applied to predict the composition of fumaroles using the Keeling method. The direct measurement of isotopic CO_2 in a volcanic plume is promising for the development of CRDS as monitoring tools on volcanoes with open vent degassing where vents are inaccessible for direct sampling. Isotopic variations in atmospheric CO_2 were also detected during plume measurements. For future application of the CRDS, plume samples should always be taken at the same time of day to allow for inter-comparison of data. Overall, CRDS facilitate the rapid collection of isotopic data allowing for broader sampling of gases and faster analysis, a development that will facilitate real-time monitoring of isotopes on active volcanoes.

Résumé

Les études sur la composition isotopique du dioxyde de carbone sont utiles pour la compréhension des mécanismes de dégazage des volcans actifs. La signature isotopique de CO_2 conserve l'information selon les processus qui gouvernent la composition du magma et son histoire de dégazage. Les spectromètres de cavité anneau-bas (SCAB) portables nouvellement développés, ayant la capacité d'effectuer les mesures isotopiques, modifient la façon dont les études isotopiques sont conduites, et permettent la surveillance de CO_2 isotopique sans la préparation et le temps d'analyse requis pour le spectromètre de masse traditionnel. Les spectromètres de cavité anneau-bas, ayant été originalement développés comme instruments atmosphériques, sont maintenant utilisés comme outils afin de surveiller les gaz volcaniques. Toutefois, ces instruments n'étaient pas originalement testés dans les environnements acides et chauds, conditions similaires à celles des volcans actifs, dans lesquelles ont déjà été notées des interférences avec les SCAB. Des expériences de laboratoire ont révélé que le sulfure d'hydrogène a une interférence spectrale significative avec les lignes spectrales de ^{12}C et ^{13}C du SCAB, ce qui mène à des mesures erronées de $\delta^{13}C$ avec les concentrations de H_2S excédant 10 ppb. Afin d'utiliser ces instruments sur les volcans, où les concentrations de H_2S peuvent excéder 20 ppm, un filtre en cuivre peut être employé afin de retirer la composition entière de H_2S comprise dans les échantillons gazeux, sans affecter les valeurs de $\delta^{13}C$. D'ailleurs, en comparant les mesures de carbone isotopiques du SCAB prises en temps presque réel avec les mesures standard prises avec les spectromètres de masse à rapport isotopique (SMRI), nous observons que le SCAB enregistre des valeurs de $\delta^{13}C$ qui sont comprises dans la marge d'erreur du SMRI. Des mesures complémentaires ont été faites avec le SCAB et le SMRI au

volcan Turrialba, situé au Costa Rica, afin de caractériser la signature isotopique de ce volcan à l'activité ascendante et illustrer l'application du SCAB à l'étude isotopique des volcans. La composition isotopique de CO_2 des gaz souterrains, de la plume volcanique et des orifices à haute température révèle l'hétérogénéité de la signature isotopique de Turrialba. La modification de la signature magmatique semble être due à l'interaction avec un système hydrothermique superficiel qui neutralise le $\delta^{13}C$ vers des valeurs davantage enrichies. Les gaz contenus dans les orifices à haute température préservent une signature isotopique inchangée, ce qui supporte le concept d'un magma partiellement dégazé sous Turrialba. Les mesures de plume isotopiques effectuées avec le SCAB ont été utilisées pour prédire la composition des fumerolles en utilisant la méthode de Keeling. La mesure directe de CO_2 isotopiques dans une plume volcanique est prometteuse pour le développement des SCAB en tant qu'outils de surveillance au sein des volcans avec dégazage à orifice ouvert, où les orifices sont inaccessibles pour un échantillonnage direct. Les variations isotopiques dans le CO_2 atmosphérique ont aussi été détectées lors de mesures de la plume. Lors d'applications futures des SCAB, les échantillons de plume devraient toujours être prélevés au même moment de la journée, afin de permettre l'inter-comparaison des données. En somme, les SCAB allouent la collection rapide des données isotopiques, ce qui permet un échantillonnage davantage détaillé des gaz et une analyse plus rapide, facilitant ainsi la surveillance en temps réel des isotopes des volcans actifs.

Preface

The following thesis presents original work conducted by the author at the McGill University Department of Earth & Planetary Sciences in the 2013-2015 academic year. This work is presented as two articles submitted for publication in peer-reviewed journals of which the author is the main contributor. The first manuscript is titled *H_2S interference on CO_2 isotopic measurements using a Picarro G1101-I cavity ring-down spectrometer* and is co-authored by John Stix, Aaron Van Pelt and Gregor Lucic. The second manuscript is titled *Carbon isotope systematics of Turrialba volcano, Costa Rica, using a cavity ring-down spectrometer* and is co-authored by John Stix, Maarten de Moor, Barbara Sherwood-Lollar, Katrina Chu and Georges Lacrampe-Couloume. Fieldwork, sample preparation, data collection, and interpretation were conducted by the author under supervision of Professor John Stix. All co-authors have provided a significant level of guidance and scientific advice, or were instrumental in the collection and analysis of the data presented.

Acknowledgements

I would foremost like to thank Professor John Stix for his continual support throughout my time at McGill University. His guidance throughout my project and encouragement for personal development set him apart as an exceptional supervisor, and I was very glad to have been his student. I would also like to thank Diane Henano and all the MAGNET researchers and trainees for enriching my experience in the wonderful world of geochemistry. This network helped broaden my view of geochemistry and gave me valuable experience that will benefit me in my future. Maarten de Moor, Aaron Van Pelt, Barbara Sherwood-Lollar, Gregor Lucic, Katrina Chu and Georges Lacrampe-Couloume were all instrumental to this project. I enjoyed working with all of you and learned so much from our brief time spent together. I would like to thank Vanessa Masson for her wonderful help and patience while translating the abstract of this thesis. Thank you to the staff at the Department of Earth and Planetary Sciences, Brandon Brae, Kristy Thorton, Angela DiNinno and Anne Kosowski, for always providing much needed administrative help to students trying to maneuver the bureaucracy of the academic system. The wonderful Colin Rowell was the best companion and my biggest supporter throughout my masters. I would like to thank my parents, Natalie and Larry Malowany for the persistent and unwavering support from afar. I know that nothing I have accomplished would have been possible without you. Finally, I would like to send love out to my Montreal family, Lucas Kavanagh, Ichiko Sugiyama, Brandon Brae, Peter Crockford, Naomi Barshi, Gregor Lucic, Charlie Beard and Rowan Wollenberg for inspiring me with your own ambitions and being the greatest friends.

Table of Contents

List of Tables

List of Figures

Chapter One: General Introduction

CO_2 plays a significant role in global climate change due to the continual increase in its atmospheric composition since the industrial revolution (Keeling et al.,1995). Persistent efforts have been made to characterize the carbon budget of the earth to better understand the carbon sources and sinks on our planet. CO_2 outgassing from volcanoes is a major natural source of CO_2, but the actual amount of carbon released at volcanoes remains poorly constrained (Wallace 2005; Burton et al. 2013; Aiuppa et al. 2014). Isotopes are powerful tool for investigating natural process that alter the isotopic signature of CO_2, which are directly or indirectly linked to magmatic activity and other environmental processes.

Carbon isotope studies have been conducted on active volcanoes to understand the process of magma degassing (Gerlach and Taylor 1990) and to predict the magma source composition (Sano and Marty 1995). The traditional approach for analyzing carbon isotopes by isotope ratio mass spectrometry (IRMS) makes the use of carbon isotopes as a monitoring tool challenging and labor intensive. Recently, the development of portable instruments capable of measuring isotopic compounds in real-time or near-real time (O'Keefe and Deacon, 1998) have provided a new tool for continuous real-time monitoring of volcanic gases. Portable cavity ring-down spectrometers (CRDS) were originally designed as atmospheric instruments to monitor the rise in atmospheric CO_2 concentrations (Crosson 2008; Chen et al. 2010), but they have become popular in many fields for their simple and efficient method of measuring stable isotopes. These instruments have only recently been adapted for volcanic environments (e.g. Lucic et al. 2015). This work tests the application of CRDS on active volcanoes to validate its use as a potential monitoring tool, to facilitate rapid and robust measurements, and to provide insight into degassing mechanisms and CO_2 sources at volcanoes.

Cavity ring-own spectrometers operate using absorption spectroscopy to measure the abundance of carbon's two most abundant isotopologues (^{12}C and ^{13}C). Every small gas-phase molecule has unique absorption spectra, and can be easily distinguished in the near-infrared. In practise, a single frequency laser with a wavelength which corresponds to the unique vibrational frequency of the target isotopologue (e.g. $^{12}C^{16}O_2$) is shot through a vacuum-filled cavity. The laser bounces between mirrors in the cavity over a path length of 20 km until it reaches threshold intensity. At which point, the laser is abruptly turned off and the target gas is introduced into the cavity. Subsequent energy loss is measured using a photodetector. The 'ring-down' measures the time it takes for the intensity to drop to background levels. Accelerated energy loss is attributed to the presence of the target species which are absorbing energy faster than would normally be lost in an empty cavity. Depending on the absorption spectra, we can determine which molecules are absorbing energy and their respective concentrations when comparing them to well characterized standard with a known composition. The comparative method produces precise and robust measurements which are repeated every 10 seconds. Typical sample run times will be 10 – 20 minutes in order to obtain a statistically significant sample size for the measurements.

The CRDS were originally developed for measuring ambient atmosphere, and monitoring changes in the global CO_2 budget. Volcanic environments can have very different gas compositions than those found in ambient atmosphere; thus for its implementation on volcanoes, we must first evaluate the performance of the CRDS under volcanic conditions. Previous work by Lucic et al. (2015) alluded to interference caused by large quantities of H_2S found in certain gas samples. The first part of this thesis presents a series of experiments conducted to characterize the interference of H_2S upon a G1101-i CRDS from Picarro Inc. and proposes a technique for removing H_2S from gas samples without altering their isotopic composition. This is

extremely important for the implementation of CRDS on volcanoes where H_2S is a major gas species. There are other interferences which exist with the CRDS, such as elevated water concentrations (Rella et al. 2013), methane (Vogel et al. 2013), and changes in the background noble gas chemistry (Nara et al. 2012). These interferences are not addressed in this work, but it is important to be aware of all possible sources of error for when implementing CRDS in a new environment. To address any unforeseen interference in our data, we have compared all CRDS field-based measurements with duplicate IRMS measurements. This has identified samples where interference with the CRDS arises, and suggests new avenues for research when applying CRDS on active volcanoes.

The second part of this work is a comprehensive characterization of the carbon isotope composition of gases on Turrialba, Costa Rica, an active volcano in the Central American Volcanic Arc. Previous isotope studies reveal increasing activity at Turrialba since the 1990's (Vaselli et al. 2010; Hilton et al. 2010; Shaw et al. 2003), and a comprehensive study serves to resolve subtle differences in the isotope signature resulting from the recent changes in volcanic activity there. Ash eruptions beginning on October 31st, 2014 highlight a new phase of activity, and isotope studies can help further our understanding of the degassing state of the magma that supplies Turrialba. The CRDS allows for the characterization of gases in near-real time and is highly sensitive to low CO_2 concentrations, making it useful as tool in the surveillance of volcanic activity. In a short period from April 1st-6th, 2014, a comprehensive study was undertaken of the carbon isotopes, including the use of the CRDS to make measurements of the volcanic plume. $^{13}C/^{12}C$ plume measurements have been able to reproduce the volcanic carbon isotope composition, by modeling the gas as a mixture between the volcanic and atmospheric components (Chiodini et al. 2010). Plume gases can be directly measured and are easily

extrapolated to characterize the magmatic source composition. With the capacity of the CRDS to make measurements in near real-time, we can translate plume measurements into real-time evaluations of the carbon isotope composition on a degassing volcano. This can also be compared to the fumarole and vent emissions on the volcano to estimate which processes influence the degassing signature. Portable instruments are extremely valuable as monitoring tools by making quick assessments of a volcano's activity. They also facilitate isotopic studies by reducing the time and cost associated with laboratory analysis. This work lays a foundation for deploying CRDS on active volcanoes and provides an example of applying isotopes to extract key information for understanding a magmatic system.

Preface to Chapter Two

Monitoring volcanic gas compositions can be challenging on active volcanoes where conditions are adverse to instrumentation due to anomalous concentrations of acidic gases and extremely high temperatures. CRDS instruments have not been extensively tested under these conditions, and there is thus a need to anticipate times when the instrument is unable to make accurate measurements. Early studies using the CRDS at Long Valley Caldera, California, identified an anomalous response of δ13C values in locations that had H2S in the gas phase (Lucic et al. 2015). Collaboration with Picarro Inc., the manufacturer of the G1101-i CRDS, confirmed that the CRDS had an interference with H2S. A laboratory study was conducted to characterize this interference and test a method for removing H2S without altering the δ13C composition of the gas. Chapter Two details the laboratory tests undertaken to quantify the interference using a series of standard gases spiked with H2S. The results from this study will aid in the application of CRDS in volcanic environments where H2S is present.

Chapter Two: H_2S interference on CO_2 isotopic measurements using a Picarro G1101-i cavity ring-down spectrometer

Kalina Malowany[1], John Stix[1], Aaron Van Pelt[2] and Gregor Lucic[1]

[1] Department of Earth & Planetary Sciences, McGill University, Montreal, Canada

[2] Picarro Inc., Santa Clara, USA

Correspondence to: K. S. Malowany (kalinamalowany@mail.mcgill.ca)

Abstract

Cavity ring-down spectrometers (CRDS) have the capacity to make isotopic measurements of CO_2 where concentrations range from atmospheric (~400 ppm) to 6,000 ppm. Following field trials, it has come to light that the spectrographic lines used for CO_2 have an interference with elevated (higher than ambient) amounts of hydrogen sulfide (H_2S), which causes significant depletions in the $\delta^{13}C$ measurement by the CRDS. In order to deploy this instrument in environments with elevated H_2S concentrations (i.e., active volcanoes), we require a robust method for eliminating this interference. Controlled experiments using a Picarro G1101-i optical spectrometer were done to characterize the H_2S interference at varying CO_2 and H_2S concentrations. The addition of H_2S to a CO_2 standard gas reveals an increase in the $^{12}CO_2$ concentration and a more significant decrease in the $^{13}CO_2$ concentration, resulting in a depleted $\delta^{13}C$ value. Reacting gas samples containing H_2S with copper prior to analysis can eliminate this effect. However, experiments also revealed that the addition of H_2S to CO_2 results in the formation of carbonyl sulfide (OCS) and carbon disulfide (CS_2), causing a decrease in the overall CO_2 concentration without affecting the $\delta^{13}C$ value. It is important for future work with CRDS,

particularly in volcanic regions where H_2S is abundant, to be aware of the H_2S interference on the CO_2 spectroscopic lines and to remove all H_2S prior to analysis. We suggest employing a scrub composed of copper to remove H_2S from all gas samples that have concentrations in excess of 1 ppb.

2.1 Introduction

Cavity ring-down spectroscopy (CRDS) is a relatively new method for making isotopic measurements of carbon dioxide, methane and water vapor at atmospheric concentrations(O'Keefe and Deacon, 1988). Applications for instruments using CRDS include monitoring of greenhouse gas emissions (Chen et al., 2010; Crosson, 2008), monitoring carbon storage and sequestration (Krevor et al., 2010), studying plant respiration (Cassar et al., 2011; Munksgaard et al., 2013), and process monitoring in the automotive and pharmaceutical industries (Gupta et al., 2009). Recent attempts to apply this technique to monitoring of active volcanic centers have been successful (Lucic et al., in review, 2014; Malowany et al., 2014), but in some instances there have been anomalous responses from the Picarro G1101-i CRDS. Volcanoes emit a range of gases whose concentrations can be much higher than their concentrations in the ambient atmosphere. In particular, hydrogen sulfide gas is abundant in certain volcanic centers, and can produce interference in the near infrared spectrum in which the instrument operates. Our goal was to characterize and quantify this interference for future applications of the CRDS in volcanic environments.

Carbon isotopes are powerful tracers of volcanic gases and degassing processes (Gerlach and Taylor, 1990; Taylor, 1986) and are currently analyzed with a suite of other geochemical tracers to monitor activity at active volcanoes (Carapezza et al., 2004). CRDS has a promising future monitoring activity at volcanic centers and tracking real-time changes in the isotopic

composition of volcanic gases. However, interference of H_2S with the isotopes of carbon dioxide prevents accurate measurements of the $^{12}CO_2$ and $^{13}CO_2$ concentrations, resulting in erroneous $\delta^{13}C$ measurements. To use CRDS at volcanic centers, the interference of H_2S gas needs to be characterized and removed. This paper reports the results of laboratory tests using carbon dioxide of a known isotopic composition spiked with different amounts of H_2S to assess the nature of the H_2S interference upon the CRDS. These controlled experiments were designed to qualitatively and quantitatively characterize the interference of H_2S from low concentrations (1 ppb) to those observed at volcanic centers (> 10,000 ppb). To use these instruments for in situ measurements, a quick and efficient way of removing H_2S from the sample gas prior to analysis is needed. Metals which have a high affinity for acid species, such as copper and zinc, react rapidly with H_2S to form metal sulfides. If H_2S can be removed from a sample gas without altering the isotopic composition of carbon dioxide, then the successful application of CRDS in H_2S – rich environments will only require application of a simple metal scrub prior to analysis.

2.2 Methodology

2.2.1 Experimental setup

Lab experiments were implemented to test the response of a cavity ring-down spectrometer over a range of H_2S concentrations, and then remove all traces of H_2S using a copper scrub. A Picarro G1101-i cavity ring-down spectrometer, S/N CBDS-086, designed for measuring the isotopic concentration of CO_2, was set up in a lab at ambient conditions (25º C, altitude = 100 m.a.s.l., and a summer humidity index of 60-78). The instrument performs continuous measurements while in operation, and samples are run in series, always returning to background values between measurements. This instrument has an intake valve connected to a

Tedlar® gas bag containing a mixture of CO_2 and H_2S gas. The internal pump in the CRDS actively pumps the gas at 30 mL/min into its cavity. Each gas mixture was first run directly into the instrument to observe the H_2S interference at different H_2S and/or CO_2 concentrations, and then it was run through 10 cm of copper tubing containing copper filings before entering the instrument (Figure 1). Copper readily reacts with the H_2S, removing it from the gaseous phase and leaving the pure CO_2 to be analyzed by the instrument. Copper filings were added to the copper tube to increase the surface area of copper available to react with the H_2S. Both the Tedlar® gas bags and the Tygon® tubing used in these experiments are semi-permeable to CO_2; therefore, samples were prepared immediately prior to analysis to minimize the effects of diffusion.

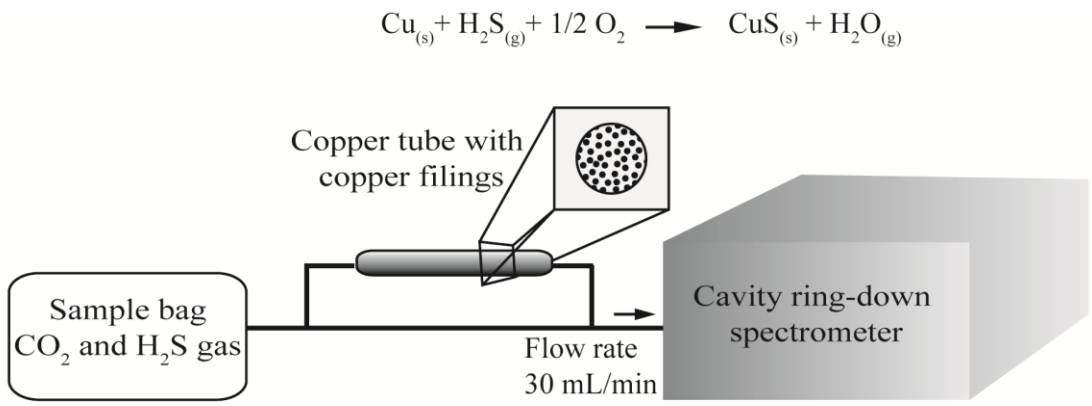

Figure 1: Diagram showing the H_2S experimental setup. A sample bag containing a standard gas with known CO_2 concentration and isotopic composition was spiked with various amounts of H_2S. The gas mixture was run directly into the CRDS to observe the interference, and then it was run through a copper tube filled with copper filings to ensure

that H_2S was removed and the isotopic value returned to that of the standard. Copper reacts with hydrogen sulfide, precipitating copper sulfide and releasing water. This can be observed by an increase in the water content measured by the CRDS after a sample has been run through the copper apparatus. A small decrease in the $^{12}CO_2$ and $^{13}CO_2$ concentrations is thought to result from the formation of small amounts of carbon disulfide and carbonyl sulfide resulting from the reaction of H_2S with CO_2 in the sample bag.

2.3 Gas mixture

Gas samples were prepared using mixtures of H_2S, CO_2 and CO_2 - free air. A standard CO_2 gas of 995 ppm and isotopic composition of -28.5‰ was spiked with different volumes of a 100 ppm H_2S gas to give H_2S concentrations ranging from 1 ppb to 20,000 ppb (20 ppm). Dilutions were performed such that the CO_2 standard was not diluted to less than 900 ppm and yielded at least one litre of gas mixture. A second suite of gas mixtures comprised varying concentrations of both CO_2 and H_2S to illustrate the effect of H_2S upon different CO_2 concentrations. A 100% CO_2 standard gas with an isotopic value of -16.0 ‰ was diluted to 500 ppm, 1,000 ppm, 2,000 ppm and 3,000 ppm by adding air that had been scrubbed using ascarite (NaOH) to remove background CO_2. The diluted gas was then spiked with 100 ppb, 200 ppb or 300 ppb H_2S. CO_2 concentrations were maintained at concentrations less than 3,000 ppm because the instrument is not designed for CO_2 concentrations higher than this. H_2S can generate interferences at concentrations less than 20 ppb, hence samples were run at H_2S concentrations of 1 – 20,000 ppb (20 ppm).

2.4 Procedure

Prior to the start of every set of analyses, the CO_2 standard gas was analyzed to monitor instrumental drift and to use as a baseline for the subsequent analyses. A sample was run on the instrument by attaching a gas bag using Tygon® tubing and allowing the CRDS to pump gas into the intake. Between measurements the instrument measured the background atmosphere composition (~ 500 ppm), but when a sample bag was attached, there was an increase in the CO_2 concentration to 995 ppm. At this concentration level, the samples have lower instrumental noise than the background measurements. In order to obtain a reliable measurement, the gas bag was measured for 10 – 15 minutes. Using the statistical tools of the spectrometer's interface, the $\delta^{13}C$ value of the gas sample was averaged using the raw delta value for the duration of the sample analysis. This yielded a time-averaged measurement of the isotopic composition, as well as the $^{12}CO_2$ and $^{13}CO_2$ concentrations. The instrument also measures H_2O and CH_4 concentrations continuously.

After a CO_2 gas sample spiked with H_2S was analyzed, the sample bag was removed, and the instrument was allowed to return to background values. High H_2S concentrations can cause large interferences with the isotopic measurements, and it sometimes took time to return to background $\delta^{13}C$ values, even after CO_2 concentrations had stabilized at ambient levels. After returning to background, the same sample was again connected to the instrument using Tygon® tubing, then run through a copper tube filled with copper filings before entering the instrument. This procedure removed all H_2S and allowed the instrument to measure the CO_2 gas without any interference from H_2S. Data collection was similar to the previous run; the sample bag was analyzed for 10 – 15 minutes, and then the instrument was brought to background values. With H_2S removed, the instrument was able to return to background levels of $\delta^{13}C$ and CO_2 quickly. A

single 10 cm tube of copper filled with copper filings was used for all analyses, and was effective for all H_2S concentrations. Other trials (not included here) have shown that repeated measurements at H_2S concentrations in excess of 1 ppm should use more copper (i.e. longer tube and more filings) than used for these experiments. The deposition of copper sulfide on the filings is a good indication of the efficiency of the scrub; once a large portion of the copper is visibly reacted, the scrub should be changed.

2.5 Results

Interference was first observed with the addition of 20 ppb H_2S, causing a change in $\delta^{13}C$ of -0.5 ‰ from the 995 ppm CO_2 standard ($\delta^{13}C$ = -28.5‰). As H_2S concentrations increased, the $\delta^{13}C$ decreased proportionally (Figure 2). A sample without H_2S returned a stable $\delta^{13}C$ value, but with increasing amounts of H_2S the $\delta^{13}C$ value started to decrease over the course of a single run. This resulted in an increasingly negative slope in the raw $\delta^{13}C$ signal with the addition of greater amounts of H_2S.

The decrease in the measured $\delta^{13}C$ resulted from changes in the $^{12}CO_2$ and $^{13}CO_2$ concentration measurements in the presence of H_2S. Figure 3 shows an increase in the $^{12}CO_2$ concentration and a significant decrease in the $^{13}CO_2$ concentration measured by the CRDS when comparing samples diluted with variable amounts of H_2S to the same diluted samples that had been scrubbed of H_2S. The percent change in the $^{12}CO_2$ and $^{13}CO_2$ concentrations are represented by Eq. (1), illustrating how the addition of H_2S affects the measurements of the carbon isotopes used to calculate the $\delta^{13}C$ value:

$$\%\ \text{change in } {}^{12}CO_2 \text{ concentration} = \frac{[{}^{12}CO_{2\ \text{with H2S}} - {}^{12}CO_{2\ \text{with copper scrub}}]}{[{}^{12}CO_{2\ \text{with copper scrub}}]} \times 100 \qquad (1a)$$

$$\%\ \text{change in } {}^{13}CO_2 \text{ concentration} = \frac{[{}^{13}CO_{2\ \text{with H2S}} - {}^{13}CO_{2\ \text{with copper scrub}}]}{[{}^{13}CO_{2\ \text{with copper scrub}}]} \times 100 \qquad (1b)$$

There is a nearly 50% decrease in the $^{13}CO_2$ concentration with the addition of 20,000 ppb H_2S, whereas the $^{12}CO_2$ concentration only increases by 3.5% for the same amount of H_2S. The end result is that H_2S causes a large negative interference on the $\delta^{13}C$ value measured by the instrument, predominantly governed by a negative interference with the $^{13}CO_2$ concentration.

Furthermore, the addition of H_2S to the CO_2 standard gas to create our gas mixture resulted in an unanticipated decrease in both $^{12}CO_2$ and $^{13}CO_2$. Figure 4 shows this decrease in both the $^{12}CO_2$ and $^{13}CO_2$ concentrations when H_2S is added compared to the pure CO_2 standard gas. Dilution of the standard occurs by addition of 3 mL of H_2S to 1000 mL of the 995 ppm CO_2 standard. This should result in a decrease of $^{12}CO_2$ and $^{13}CO_2$ concentrations of only 2.9 ppm and 0.032 ppm respectively. However, the observed decreases in the $^{12}CO_2$ and $^{13}CO_2$ concentrations are much greater than the predicted dilution, 45 ppm for $^{12}CO_2$ and 0.6 ppm for $^{13}CO_2$.This is on the order of 15 times greater than the predicted dilution. Since the decrease in CO_2 concentration cannot be explained by dilution when H_2S is added, we propose that H_2S and CO_2 reacted in the gas mixture, removing some CO_2 before the analysis.

Sample analyses with H_2S concentrations from 1 to 500 ppb show a linear interference of -1‰ for every 23 ppb H_2S added (Figure 5). The interference was successfully eliminated by reacting samples with copper. Figure 6 shows a larger range of samples from 1 ppb to 20,000 ppb. The higher H_2S concentrations still show a linear interference, but the interference is smaller at -1‰ for every 37 ppb H_2S. We believe that this discrepancy is a result of diluting the

CO_2 standard gas with larger volumes of H_2S. The suite of samples from 1- 500 ppb H_2S had larger quantities of dilute H_2S added than the sample suite from 500 – 20,000 ppb. The larger

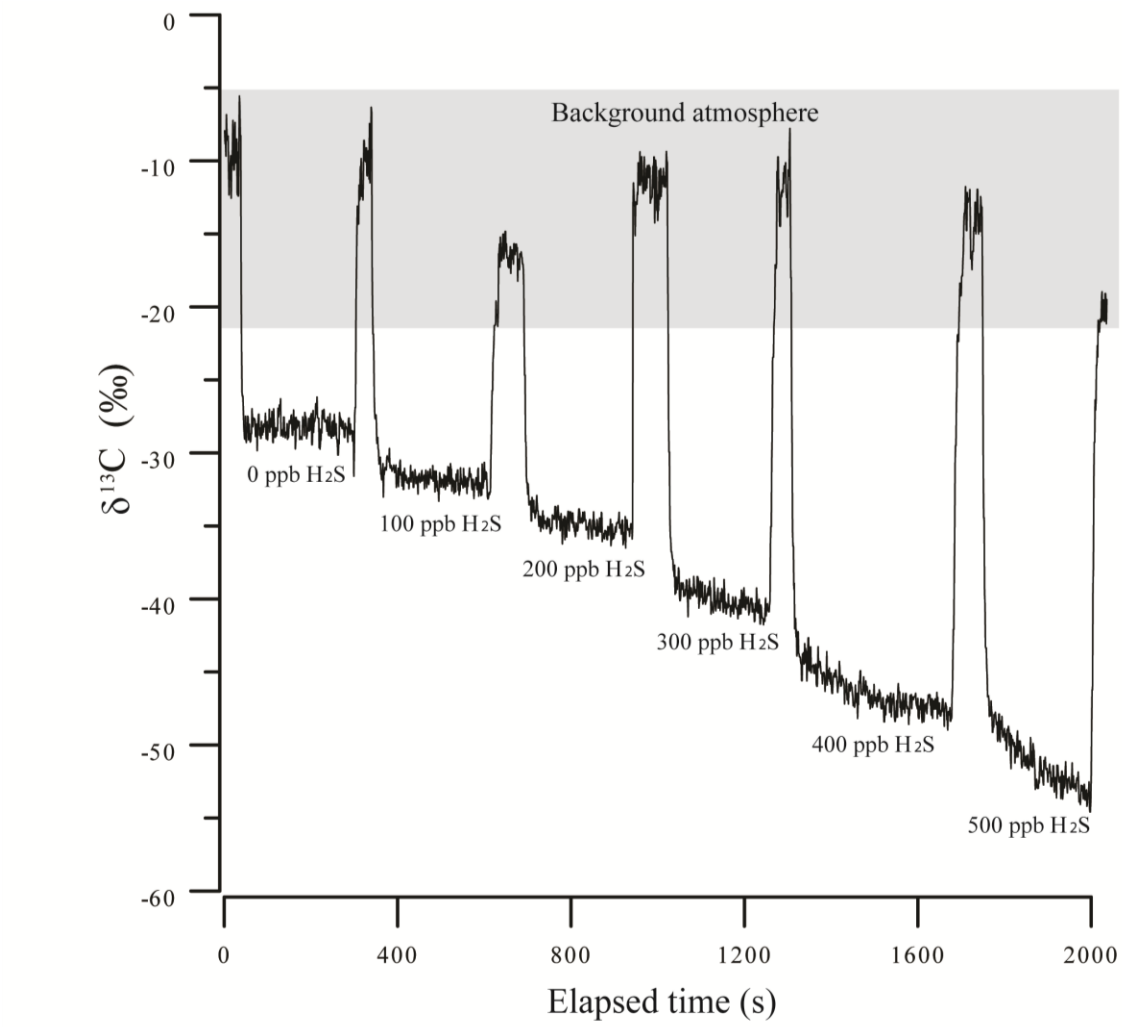

Figure 2: Raw carbon isotope signal from the Picarro G1101-i CRDS with varying amounts of H_2S. Addition of H_2S causes an increasingly negative response for the isotopic value. The raw isotopic signal at each H_2S concentration does not stabilize, but instead starts to slowly decrease resulting in a 'sloped' response. Variations in background levels can be attributed to variations in laboratory conditions (i.e., respiration).

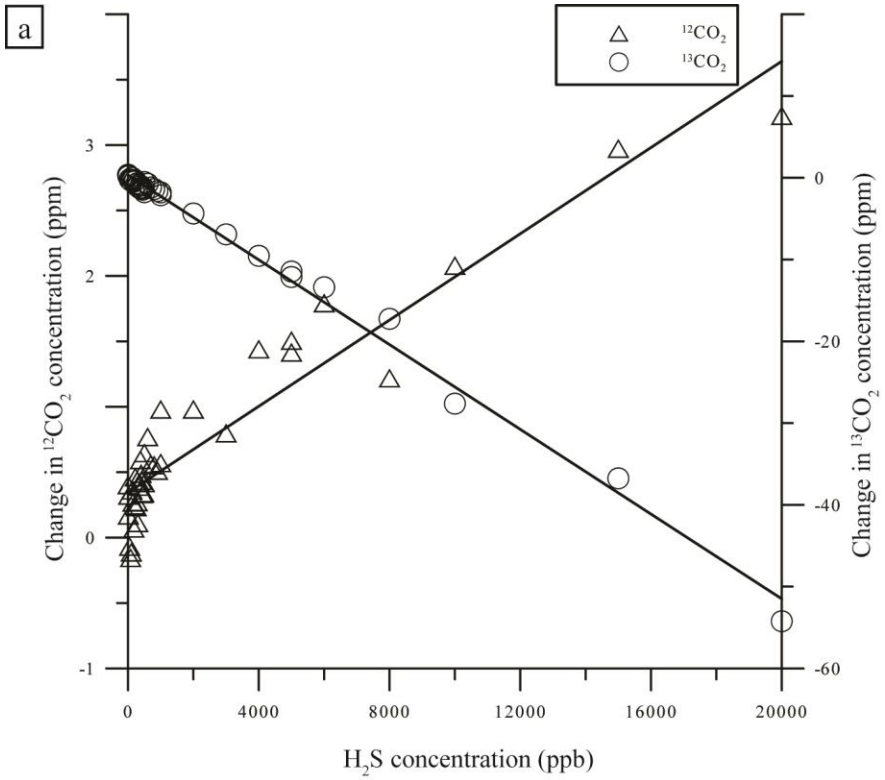
a
$^{12}CO_2$
$^{13}CO_2$
Change in $^{12}CO_2$ concentration (ppm)
Change in $^{13}CO_2$ concentration (ppm)
H_2S concentration (ppb)
3
2
0
-1
0
-20
-40
-60
0
4000
8000
12000
16000
20000

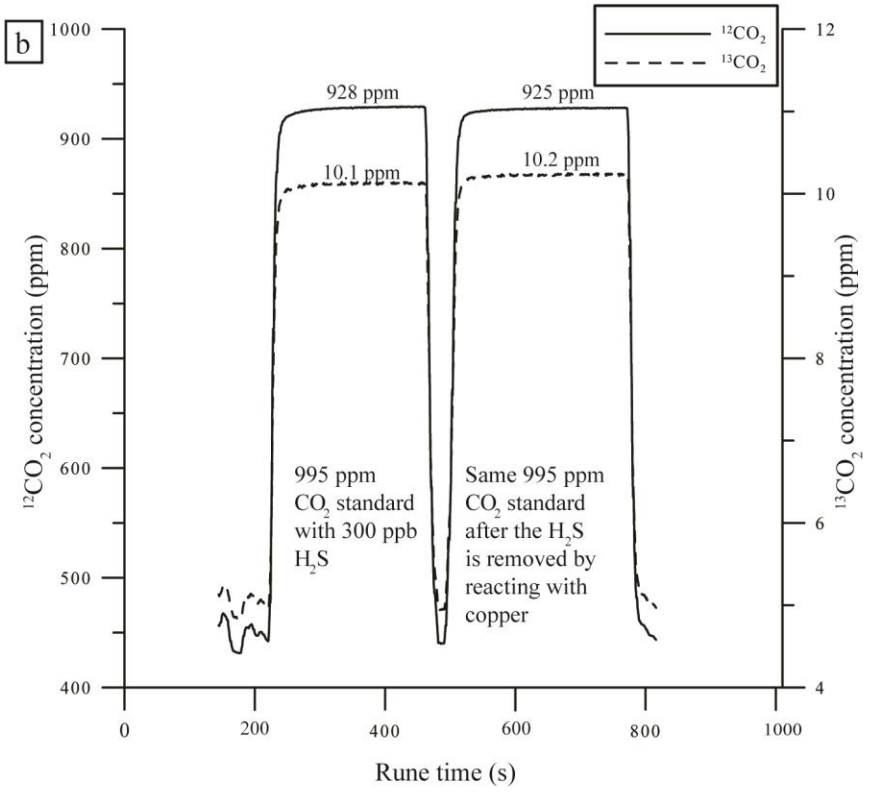
b
$^{12}CO_2$
$^{13}CO_2$
928 ppm
925 ppm
10.1 ppm
10.2 ppm
995 ppm CO_2 standard with 300 ppb H_2S
Same 995 ppm CO_2 standard after the H_2S is removed by reacting with copper
$^{12}CO_2$ concentration (ppm)
$^{13}CO_2$ concentration (ppm)
Rune time (s)
1000
900
800
700
600
500
400
12
10
8
6
4
0
200
400
600
800
1000

Figure 3: Change in the $^{12}CO_2$ and $^{13}CO_2$ concentrations with addition of H_2S to the standard gas. (a) Plot showing the percentage change in CO_2 concentration between gas with H_2S and gas scrubbed of H_2S. There is a visible increase in the $^{12}CO_2$ concentration and a decrease in the $^{13}CO_2$ concentration with addition of H_2S. The percentage decrease for $^{13}CO_2$ is significantly greater than the percentage increase for $^{12}CO_2$. (b) Plot showing the 1000 ppm standard CO_2 gas with the addition of 3 mL of 100 ppm H_2S and the subsequent response after the H_2S was removed with the copper scrub. There is a small, yet visible, increase in the $^{13}CO_2$ concentration and decrease in the $^{12}CO_2$ concentration when H_2S is removed.

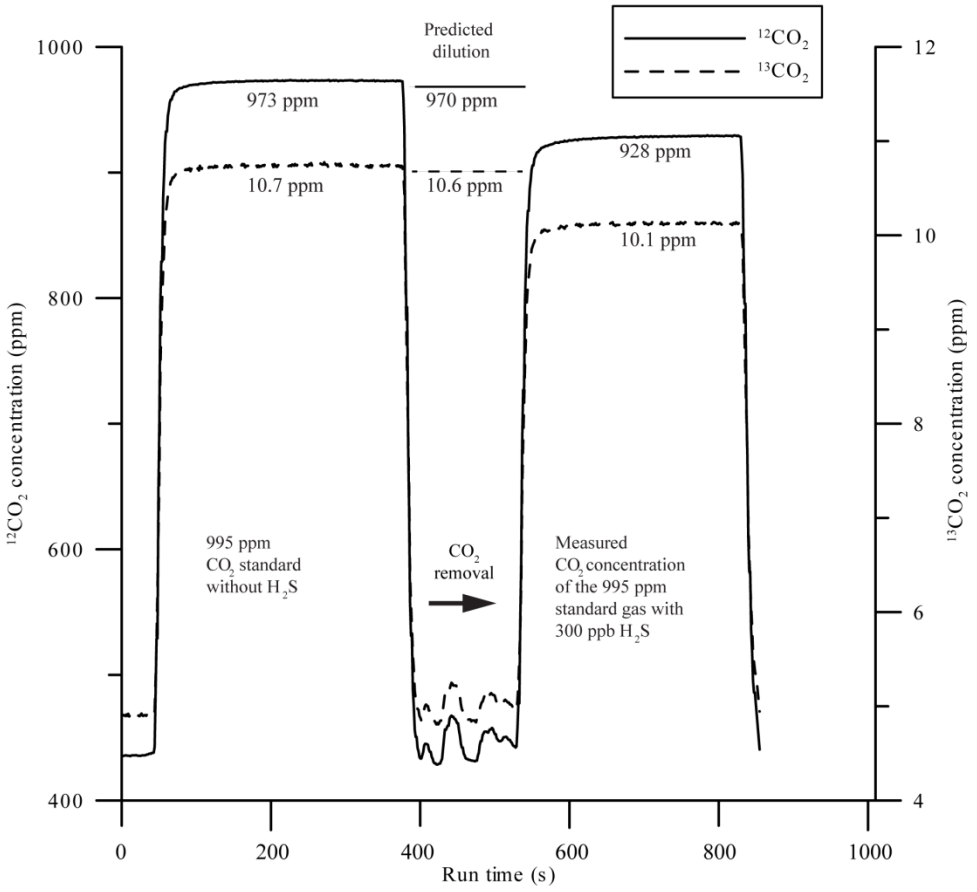

Figure 4: The addition of 3 mL of 100 ppm H_2S to 1 liter of the 1000 ppm standard gas resulted in a large drop in $^{12}CO_2$ and $^{13}CO_2$ concentrations. The observed concentrations are significantly lower than those predicted to result from dilution of the standard gas with the addition of 3 mL of H_2S. When the copper scrub removed H_2S, the CO_2 concentration remains anomalously low. It is likely that a reaction between H_2S and CO_2 removes a portion of the CO_2 from the mixture before it is analyzed.

dilutions resulted in lower CO_2 concentrations, suggesting that the H_2S interference also depends on CO_2 concentration. Hence, we ran a further series of experiments to examine this effect.

The set of experiments performed at a range of CO_2 concentrations (500 to 3,000 ppm CO_2) revealed that the H_2S interference also depends strongly on the CO_2 concentration (Figure 7). The interference from H_2S is much smaller at high CO_2 concentrations, and is quite large at atmospheric concentrations. For example, an interference of -1‰ resulted from the addition of 21 ppb H_2S at 500 ppm CO_2, whereas at 3,000 ppm CO_2 an interference of -1‰ required the addition of 154 ppb H_2S. Thus, the H_2S interference is also dependent on the CO_2 concentration of the sample. During experiments performed at a fixed H_2S concentration, it was found that the H_2S interference with $\delta^{13}C$ was inversely proportional to the CO_2 concentration of the sample. Figure 8 illustrates the variation of the H_2S interference at different CO_2 concentrations and shows this inverse relationship between CO_2 concentration and H_2S interference.

2.6 Discussion

Carbon isotopic measurements of CO_2 using cavity ring-down spectroscopy have a clear interference in the presence of H_2S that is dependent on both the H_2S and CO_2 concentrations. At lower CO_2 concentrations, the H_2S interference was more pronounced due to the relatively higher proportions of H_2S contained within the sample. This may explain the discrepancy between the slopes of Figure 5 and Figure 6, where there was more dilution of the CO_2 standard gas at lower H_2S concentration (Figure 5) than at higher H_2S concentration (Figure 6), resulting in a larger H_2S/CO_2 ratio in samples with lower CO_2 concentrations.

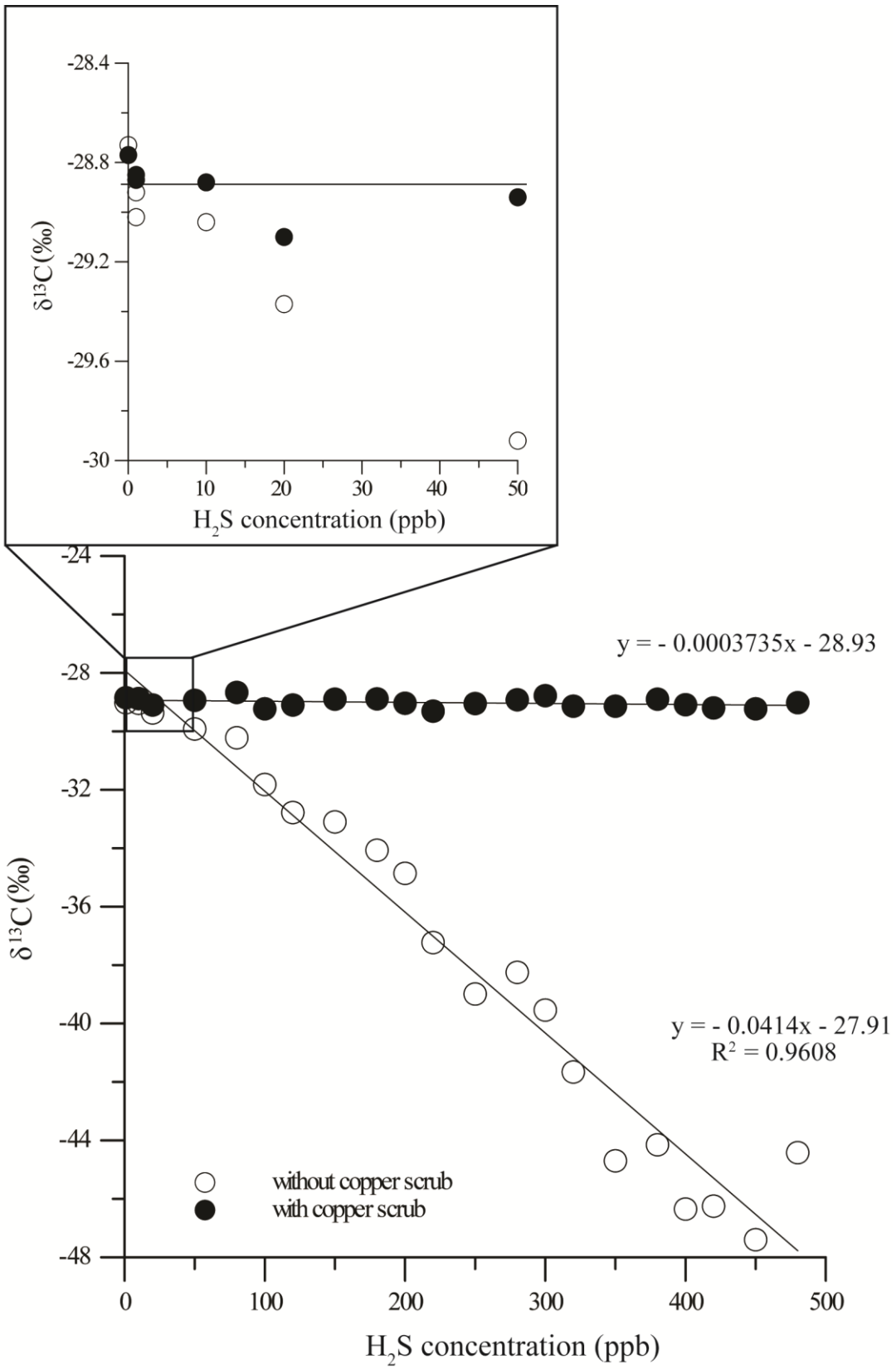
-28.4
-28.8
-29.2
-29.6
-30
δ13C (‰)
0
10
20
30
40
50
H2S concentration (ppb)
-24
-28
-32
-36
-40
-44
-48
δ 13C (‰)
y = - 0.0003735x - 28.93
y = - 0.0414x - 27.91
R2 = 0.9608
without copper scrub
with copper scrub
0
100
200
300
400
500
H2S concentration (ppb)

Figure 5: Isotopic signal from the Picarro G1101-i CRDS for 995 ppm CO_2 with H_2S concentrations ranging from 0 to 500 ppb. Black dots represent isotopic measurements after H_2S has been removed with copper; here the isotopic composition is maintained at the standard value (-28.5 ‰).

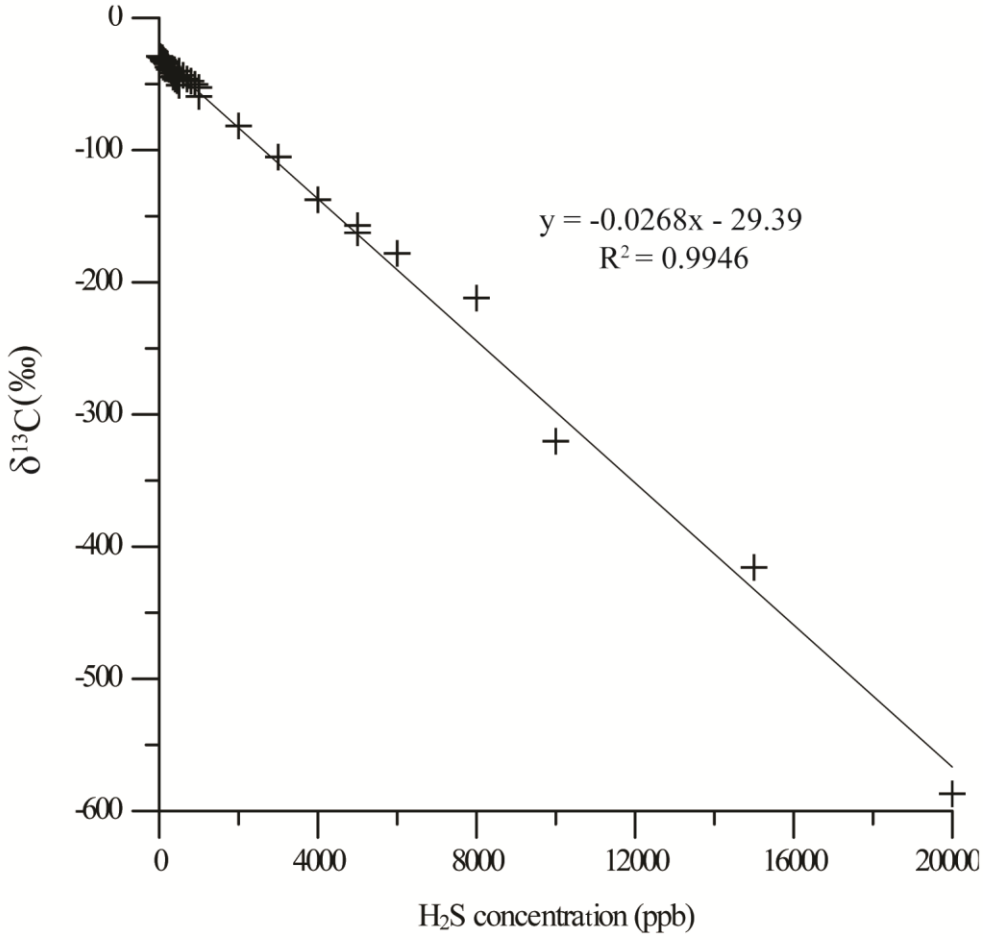

Figure 6: Isotopic signal from the Picarro G1101-i CRDS for 995 ppm CO_2 with H_2S concentrations ranging from 0 to 20,000 ppb (0 - 20 ppm).

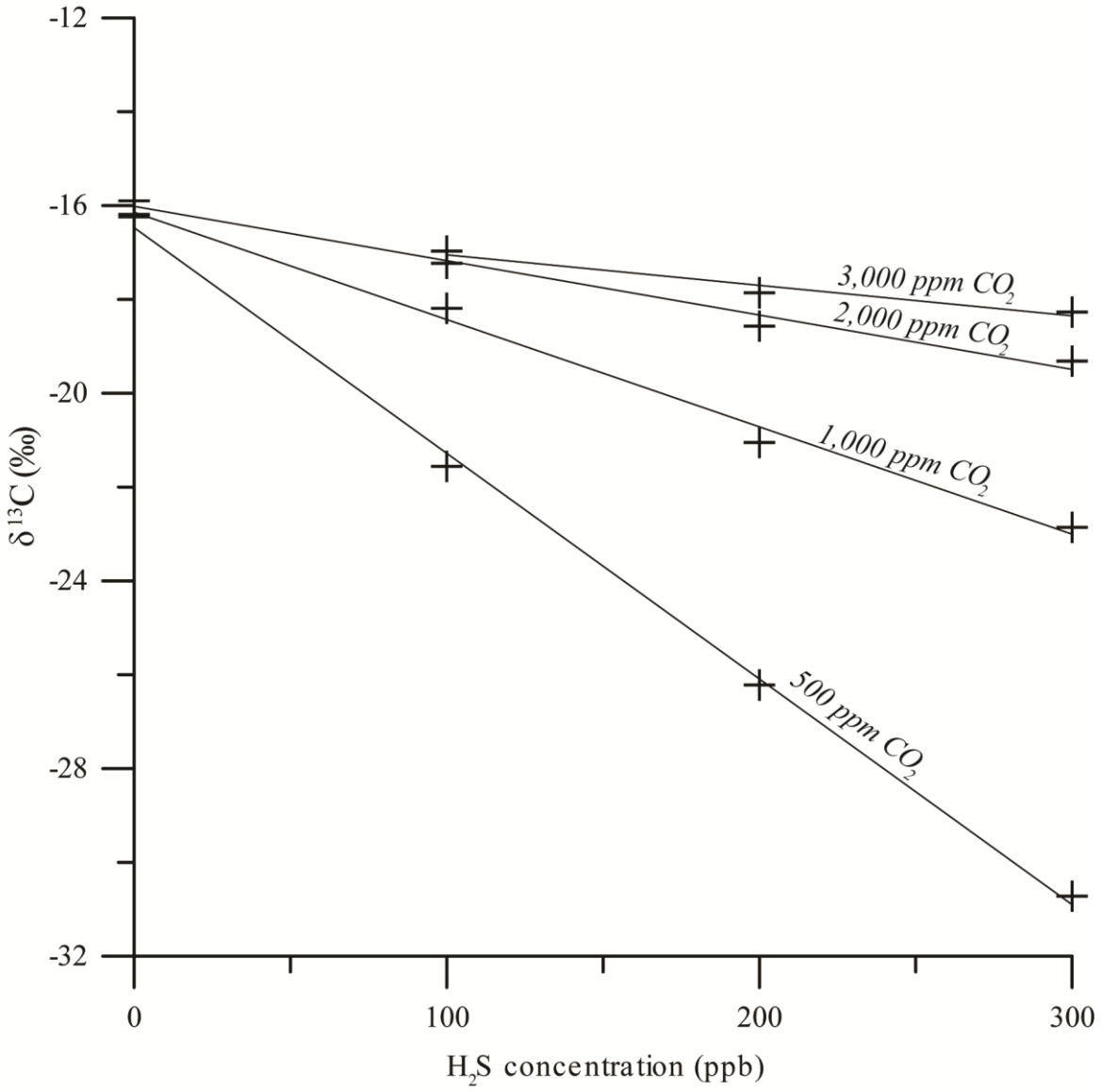

Figure 7: Changes in $\delta^{13}C$ when H_2S is added to a standard CO_2 gas (-16.0 ‰) at varying CO_2 concentrations. The H_2S interference is strongly dependent on the CO_2 concentration of the sample.

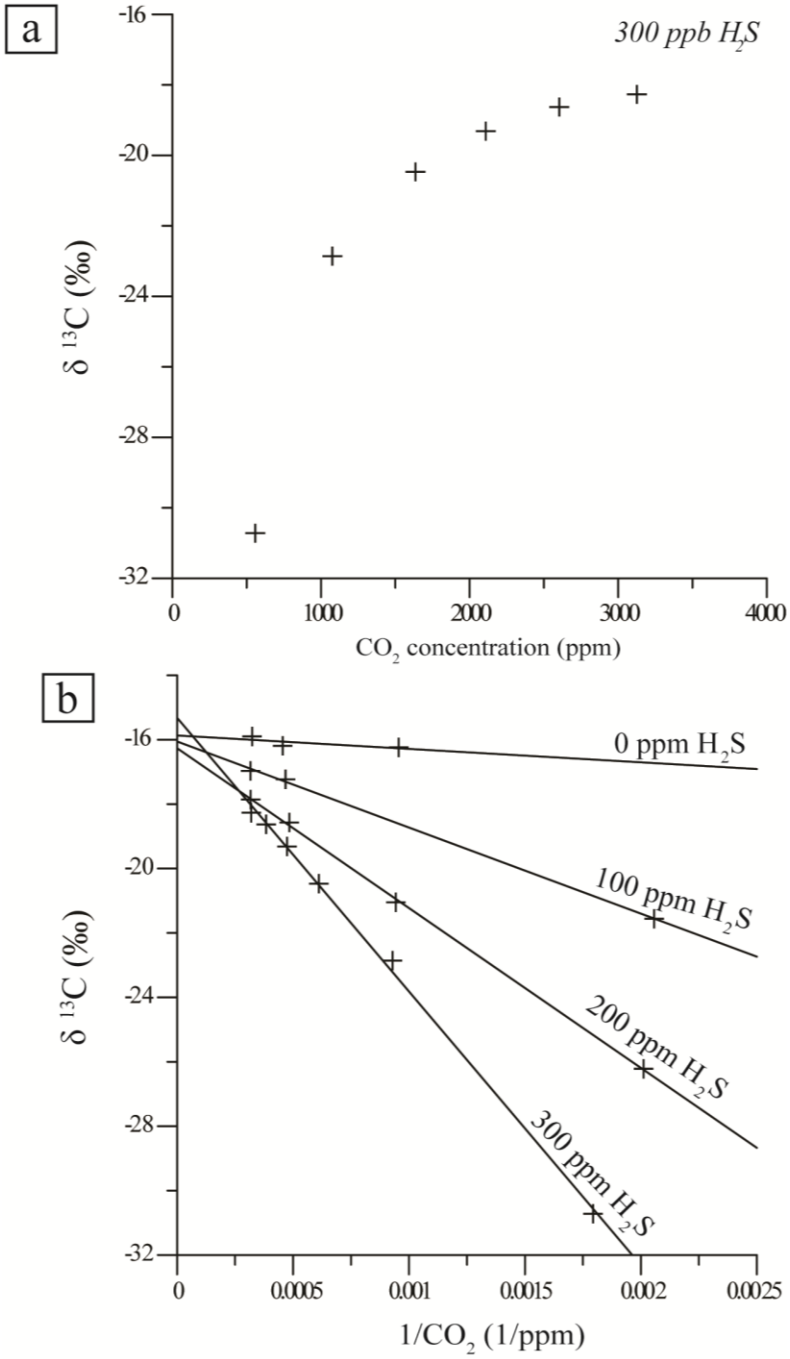

Figure 8: The H_2S interference is inversely related to the CO_2 concentration. (a) The isotopic signal from the CRDS varies with changing CO_2 concentration when the H_2S concentration is held constant at 300 ppb. (b) Isotopic value vs. $1/CO_2$ illustrating the

change in $\delta^{13}C$ with the addition of H_2S to a standard gas (-16.0 ‰) at different concentrations.

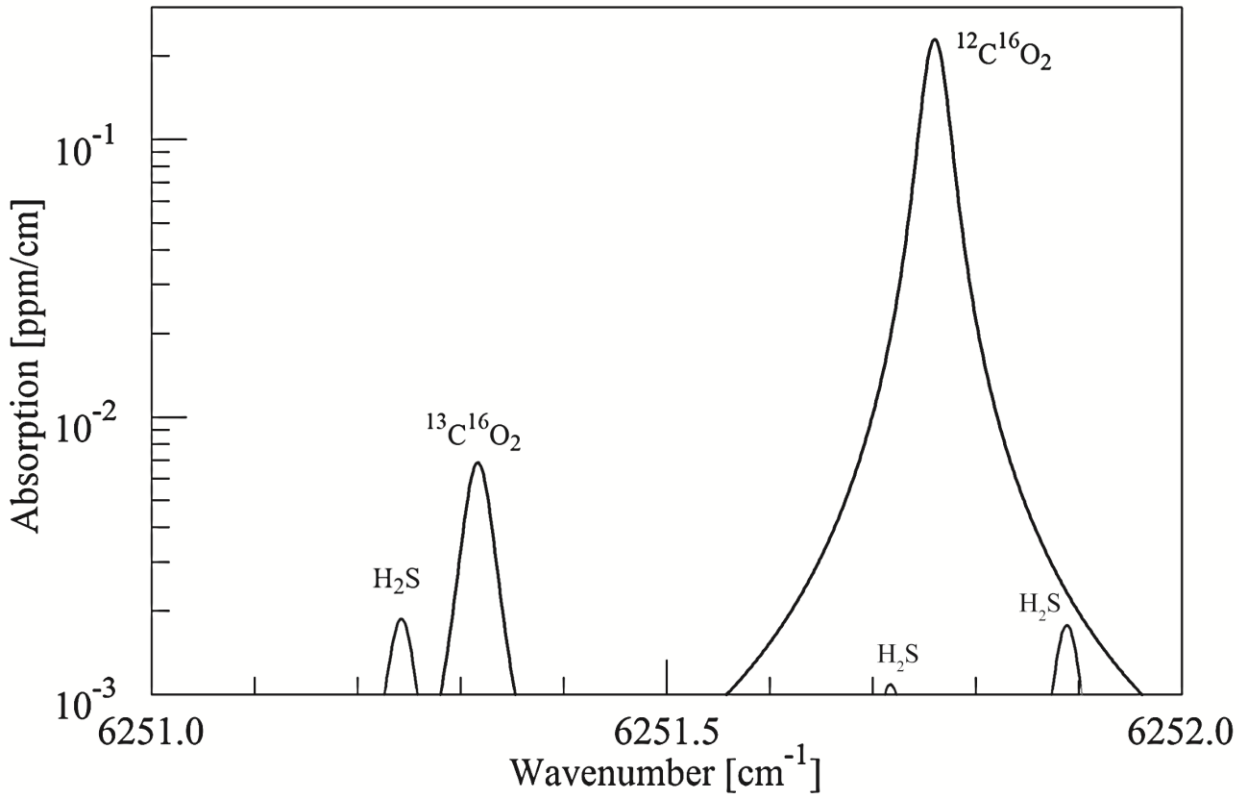

Figure 9: Hitran model for 400 ppm CO_2 and 1 ppm H_2S (45° C, 140 Torr) illustrates the overlapping of H_2S lines with CO_2 lines. The relative magnitude of H_2S interference is much larger for $^{13}CO_2$ than for $^{12}CO_2$. Note the logarithmic scale.

The H_2S interference with the G1101-i CRDS is an inherent property of the spectral lines that are fitted to determine the $^{12}CO_2$ and $^{13}CO_2$ concentrations (Figure 9). The specific spectral lines used in the Picarro G1101-i were chosen to avoid overlapping ambient levels of common gas species encountered in atmospheric air (i.e., H_2O, CH_4, NH_3, etc.). In the case of water

vapour for example, where it is not possible to choose CO_2 lines that are free from overlap, the system measures and corrects for such species to the extent that they interfere with either the $^{12}CO_2$ or $^{13}CO_2$ spectral features. For H_2S specifically, the chosen spectral lines avoid the strongly absorbing H_2S spectral lines, but there are weaker lines that partially overlap with both spectral features of the CO_2 used in the system. At typical ambient levels of H_2S for which the spectroscopy of the G1101-i was designed, these weak lines have no measureable effect on the reported CO_2 concentrations or carbon isotope ratio. However, at elevated levels, they begin to cause the observed measurement bias.

Since the isotope ratio measurements in CRDS uses ratios of the absorption peaks of the two spectral lines of the CO_2 isotopologues, it is the relative concentration of H_2S to the CO_2 that determines the effect of the H_2S on the isotope ratio (Figure 9). The more pronounced effect of H_2S on the isotope ratio at lower CO_2 concentrations is due to a weak H_2S spectral line slightly overlapping the $^{13}CO_2$ line such that when the ratio of CO_2 to H_2S concentration is low, the measured $^{13}CO_2$ line will be more affected by the H_2S since it makes up a larger proportion of the overall measured line shape. There is a similar overlapping H_2S line near the $^{12}CO_2$ peak that has a similar (but opposite sign) concentration-dependent effect on the reported $^{12}CO_2$ concentration as compared to the $^{13}CO_2$ concentration. The reason for the sign difference of these two H_2S concentration-dependent effects is related to how the independent spectroscopic fitting algorithms used for each peak to calculate the isotoplogue concentrations interpret the change in line shape imparted by the interfering H_2S signal.

In addition to the H_2S interference, there was an unanticipated decrease in both the $^{12}CO_2$ and $^{13}CO_2$ concentrations with the addition of H_2S to the standard gas that could not be accounted for solely by dilution (Figure 4). It is possible that when the two gas species are

combined, they react to form either carbon disulfide (CS_2) or carbonyl sulfide (OCS), both of which can be stable at atmospheric conditions. The suggested reactions for both species are:

$$2H_2S_{(g)} + CO_{2\,(g)} \rightarrow 2H_2O_{(vap)} + CS_{2\,(g)} \quad (2a)$$

$$H_2S_{\,(g)} + CO_{2\,(g)} \rightarrow H_2O_{\,(vap)} + OCS_{\,(g)} \quad (2b)$$

Carbon disulfide and carbonyl sulfide are also present in small amounts at actively degassing volcanoes, but relatively little effort has been put forth to characterize their concentrations (Watts, 2000). Hydrothermal systems have carbonyl sulfide concentrations on the order of 10 -100 ppb (Chiodini et al. 1991). If indeed the formation of these compounds is affecting the CO_2 concentration of our gas samples, it does not appear to significantly affect the $\delta^{13}C$ composition of the standard gas. Isotopic readings of our gas mixture indicate that the effects of the above compounds are small compared to the effects of H_2S.

2.7 Concluding remarks

Isotopic measurements using this particular implementation of the CO_2 spectroscopy in cavity ring-down spectrometers have a clear and quantifiable interference resulting from the presence of H_2S in excess of a few ppb. Laboratory experiments using controlled amounts of H_2S mixed with a CO_2 standard gas of known concentration and isotopic composition show that the interference is linear and dependent on both the H_2S and CO_2 concentrations of the sample. The H_2S interference arises as a result of the line choice for this type of spectrometer (Picarro© G1101-i), which avoids interference with other common atmospheric species such as H_2O, CH_4, NH_3, etc., but has some small lines remaining in the range of H_2S that causes the interference observed at high H_2S concentrations. The most practical approach to eliminating H_2S interference when measuring the $\delta^{13}C$ value is the use of a metal scrub, for example copper, to

remove all H_2S before the sample is run through the CRDS. Removing this interference is an important step to making real-time measurements of $\delta^{13}C$ of CO_2 with cavity ring-down spectrometers in environments with high sulfur concentrations, such as actively degassing volcanoes. Volcanoes have a range of CO_2 concentrations (400 – 1,000,000 ppm) and the H_2S interference is significant in the operational range of the CRDS (0-3,000 ppm). Therefore, the most practical approach to eliminating the interference is with a simple scrub for all samples containing H_2S in excess of 1 ppb.

Preface to Chapter Three

Previous studies have compared the $^{13}C/^{12}C$ composition of a volcanic plume to the composition of CO_2 being emitted fumaroles on Mount Etna, Vulcano, and Solfatera volcanoes in Italy (Chiodini et al. 2010). Open vent degassing on volcanoes can be difficult to access by direct sampling, and measurements of plume gas provide a safe and convenient alternative to direct measurements at volcanic vents. As plume gases travel away from the source region their concentrations become progressively more dilute until they reach atmospheric concentrations. In the case of CO_2, atmospheric concentrations are about 400 ppm. Fortunately, the CRDS was designed to make precise and accurate measurements at atmospheric concentrations, and can also detect dilute plume gases that are only several ppm above ambient concentrations. Using a sampling technique that captures gas from a plume, we can combine the $\delta^{13}C$ values and CO_2 concentrations using a Keeling plot to predict the isotopic composition of the volcanic end-member. Chapter Three presents the first attempt at using the CRDS for plume measurements and applying the Keeling method to volcanic gases.

Furthermore, a comprehensive characterization of the volcanic gases at Turrialba volcano, Costa Rica, was undertaken for comparison with the predicted composition of the volcanic source derived from the plume measurements. Soil gases from the central crater and gases from a high temperature vent are used to characterize the processes controlling carbon isotope fractionation at Turrialba. This work presents findings important for the application of CRDS to volcanic plumes, while also providing insight to processes that determine the isotopic signature of gases at Turrialba.

Chapter Three: Carbon isotope systematics of Turrialba volcano, Costa Rica, using a portable cavity ring-down spectrometer

Kalina Malowany[1], John Stix[1], Maarten de Moor[2], Barbara Sherwood-Lollar[3], Katrina Chu[3], Georges Lacrampe-Couloume[3]

[1] Department of Earth & Planetary Sciences, McGill University, 3450 University Street, Montreal, Quebec H3A 0E8, Canada.

[2] Obervatorio Vulcanológico y Sismológico de Costa Rica Universidad National, Heredia, Costa Rica.

[3] Deparment of Earth Science, University of Toronto, Toronto, Ontario, Canada.

Abstract

Portable cavity-enhanced spectrometers permit a broad characterization of the isotope composition of volcanic gases with minimal sample preparation and analysis time. We have conducted an extensive characterization and analysis of the carbon isotope signature of gases at Turrialba volcano, Costa Rica, using a portable field-based cavity ring-down spectrometer (CRDS). Over the past two decades Turrialba has shifted from a hydrothermal regime to an increasingly magmatic regime with increased degassing and eruption potential. Our results of the carbon isotope signatures of the volcanic plume, high temperature vents and soil gases reveal isotopic heterogeneity in the CO_2 gas composition at Turrialba. Variations in $\delta^{13}C$ range from -4.5‰ to -3.3‰ between the high temperature vent and low temperature soil gases. We also employed the Keeling method (Keeling, 1958) to predict the isotopic composition of the magmatic source from the compositions of the volcanic plume. The plume is dominantly sourced from fumaroles in the West crater and reveals a $\delta^{13}C$ value of -2.6±1.4‰. This is significantly

different from the composition of the high temperature 2012 vent (-4.4‰), suggesting that alteration of the magmatic signature is being modified beneath fumaroles on Turrialba. We propose that the isotope range observed at Turrialba is the result of liquid-gas phase fractionation in the presence of a hydrothermal system. The hydrothermal system appears to buffer the isotopic signature of CO_2 to values enriched in ^{13}C with increasing distance from the 2012 vent. Following our measurements, an eruption on 31 October 2014 initiated a new stage of activity at Turrialba, by expelling juvenile magmatic material. Going forward, it is important to characterize the isotopic composition of gases at Turrialba through continued monitoring of $\delta^{13}C$, especially for the high temperature vents, to characterize the state of degassing and aid in eruption forecasting. Portable instruments, such as CRDS for isotopic CO_2, will be advantageous for near real-time measurements and as a monitoring tool for forecasting volcanic eruptions.

3.1 Introduction

The isotopic composition of CO_2 gas being emitted from volcanoes is a well-established tool for understanding the degassing character of a volcano (Taylor 1986; Gerlach and Taylor 1990). Previous studies have tried to link temporal variations in carbon isotopes to the eruptive potential of a volcano by inferring periods of magma replenishment from variations in the isotopic signature (i.e., Paonita et al. 2002; Vaselli et al. 2010; Paonita et al. 2013; Fischer et al. 2015). Measurements of the $\delta^{13}C$ composition of volcanic plumes provide a link to the isotopic composition of magmatic gas without necessitating direct sampling from fumaroles or vents (Chiodini et al. 2010). The recent development of portable instruments capable of measuring isotope compounds in near real-time (O'Keefe and Deacon 1988) presents the possibility of using isotopic measurements of plume gases as a monitoring tool at active volcanoes.

Cavity-enhanced absorption spectroscopy was originally developed for isotopic measurements of atmospheric gas, and recently has been adapted for volcanic environments (Lucic et al. 2015). The successful application of isotope ratio infrared spectrometers to measure the $\delta^{13}C$ composition of CO_2 in a volcanic plume demonstrates the ability of these instruments to resolve the isotope composition of the magmatic source (Rizzo et al. 2014). In this paper, we use a cavity ring-down spectrometer (CRDS) to characterize the magmatic isotope composition of a volcanic plume by adapting the Keeling method (Keeling, 1958). The Keeling approach was originally formulated to derive the biogenic component of atmospheric CO_2 using a two-component mixing model characterized by $\delta^{13}C$ composition and CO_2 concentration. Here, we use it to represent the mixture between the volcanic source and ambient atmosphere as manifested in a volcanic plume. This approach is easy to implement in near real-time, facilitating the future application of cavity-enhanced spectrometers as forecasting tools.

Portable spectrometers permit a broad characterization of magmatic gases with minimal sample preparation and analysis time (Lucic et al. 2015). Using the procedure described in Lucic et al. (2015), we analyzed gases at Turrialba volcano, Costa Rica. We performed isotope analyses on a variety of gas types at Turrialba, including the volcanic plume, the 2012 high temperature vent, fumaroles, and soil gases. Previous carbon and helium isotope data suggest that Turrialba may have variations in the magma source composition (Hilton et al. 2010). However, major gas compositions have revealed that high temperature vents are related to a single magmatic source, and that local variations in the CO_2/SO_2 ratio and the SO_2 flux result from the drying of the hydrothermal system with increasing magmatic activity (Moussallam et al. 2014; Conde et al. 2014). We apply our $\delta^{13}C$ characterization of the Turrialba gases to assess the

variations in isotope signatures and link spatial and temporal trends to the observed activity at Turrialba.

3.2 Geologic setting

Turrialba is a basaltic andesite arc volcano in Costa Rica, formed as part of the Central American Volcanic Arc (CAVA), an expression of the Cocos Plate subducting beneath the Caribbean plate (Reagan et al. 2006; Freundt et al. 2014). Turrialba shares a plumbing system with its neighboring volcano, Irazu, and together they compose the largest stratovolcano complex in Central America (Carr et al. 1990). The volcanic arc extends from Guatemala to Costa Rica, and substantial variation in gas chemistry and magma composition has been observed resulting from differences in the along-arc structural and magmatic character (Protti et al. 1995; Shaw et al. 2003; Zimmer et al. 2004; Aiuppa et al. 2014). Turrialba is upwind of the Central Valley in Costa Rica, ~20 km from the country's densest population centers of San Jose and Cartago. Eruptions from Turrialba are of concern for their direct impact on local farmland and urban centers (Reagan et al. 2006); recent eruptions (ongoing as 2015) have had substantial impact on the local community. Turrialba has had 6 major phreatic and phreatomagmatic eruptions in the past 3400 years, with the last major period of activity ending in 1866 (Reagan et al., 2006). The active edifice has three visible craters, East, Central and West, which were formed consecutively from east to west. The West Crater was formed during the eruptive event in 1864-1866, although recent eruptive activity has obscured the walls between the West and Central craters as can be seen in Figure 10.

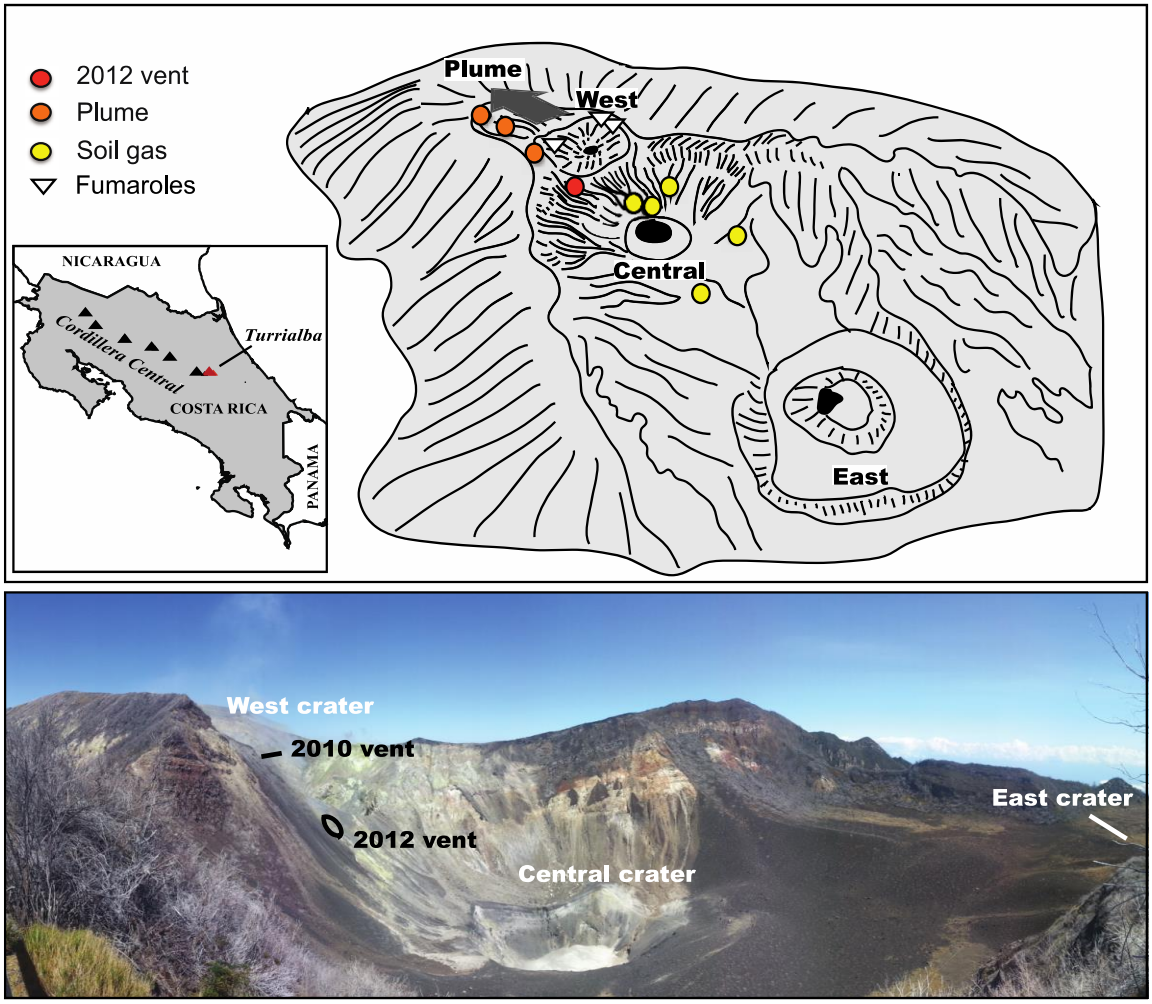

Figure 10: Turrialba volcano is part of the Central Cordilleran volcanic chain, a subsidiary of the Central American Volcanic Arc that extends north into Guatemala. There are three craters which constitute its edifice: East, Central and West. Vigorous degassing from fumaroles in the West crater comprise the majority of the plume gas. The 2012 vent is located on the flank between the Central and West crater, and emits high temperature gases (400-800°C) with a strong magmatic signature (Conde et al. 2014; Moussallam et al. 2014).

3.2.1 Recent activity

Since its last major eruption (1864-1866), Turrialba lapsed into a state of quiescence until 1996, when seismic activity commenced coupled with increased fumarolic activity at the summit, indicating a reawakening (Barboza et al. 2003). Geochemical (Tassi et al. 2004; Vaselli et al. 2010; Martini et al. 2010) and geophysical (Conde et al. 2014; Martini et al. 2010; Barboza et al. 2004) indicators suggest a progressive shift from hydrothermal-dominated to magmatic-dominated activity at Turrialba from 2001-2007 (Vaselli et al. 2010). Vent forming eruptions in 2005, 2010 and 2012 opened fractures that emitted high temperature (> 500 º C) gases (Moussallam et al. 2014; Vaselli et al. 2010). Increasing levels of degassing from the vents and fumaroles in the Central and West craters have produced sulfur deposits and generated a large visible plume (Conde et al. 2014). The plume is occasionally visible up to 2 km above the rim and follows the dominant windward direction to the west-southwest (Figure 10). As a result, the western flank of Turrialba has an extensive area of tree kill, where vegetation has been subjected to elevated levels of acid gases (Conde et al. 2014). The plume mainly comprises fumarolic gas from the west crater, with variable contributions from the 2010 and 2012 vents (Conde et al. 2014). There is a regional fault system, the Falla Ariete, which trends northeast-southwest and transects the central edifice. The most prominent surface expression of the fault is a steep canyon on the southern flank of the volcano where fumarolic activity has been observed since 2005 (Vaselli et al. 2010).

A shift from hydrothermal activity to magmatic activity dominating the gas composition at Turrialba occurred around 2007, culminating in the opening of the 2010 vent (Figure 10), after which point magmatic activity declined temporarily (Moussallam et al. 2014; Vaselli et al. 2010; Conde et al. 2013). In 2012, a second episode occurred in late January, producing the 2012 vent

and bringing high temperature gases (~ 800º C) to the surface. On October 29, 2014, an energetic summit eruption produced at the west crater eradicated the most recent vent (2012 vent) and produced ash dominated by the hydrothermally altered clasts with a minor component of juvenile magmatic material (OVSICORI, 2014). Several more ash forming eruptions occurred in late December and continued into 2015. At the time of writing (June, 2015) there have been 15 significant eruptions at the summit, and many more with minor ash emission events.

3.2.2 Geochemistry and carbon isotopes

Previous geochemical studies suggest a hydrothermal-magmatic origin of the gases at Turrialba volcano (Martini et al. 2010; Hilton et al., 2010; Vaselli et al., 2008; Tassi et al., 2004; Shaw et al., 2003). The transition between hydrothermal and magmatic conditions at Turrialba occurred between 2001 and 2007 as shown by large increases in the S_{tot}/CO_2 and $(HCl + HF)/CO_2$ ratios (Vaselli et al. 2010). $CO_2/^3He$ and $\delta^{13}C$ reported by Hilton et al. (2010) indicate variable slab contributions for the different vents at Turrialba. More recent models describe a similar magmatic source for the high temperature vent gases (2012 and 2010 vents) which are causing a progressive 'drying-out' of the local hydrothermal system (Moussallam et al. 2014). The $\delta^{13}C$ values of condensates in the Central crater (-4.8‰ to -2.2‰) are slightly more depleted than those found in the West crater (-3.4‰ to -1.4‰), suggesting that the dominant magmatic activity is closer to the Central crater, with hydrothermal activity dominating in the West crater (Vaselli et al. 2010).

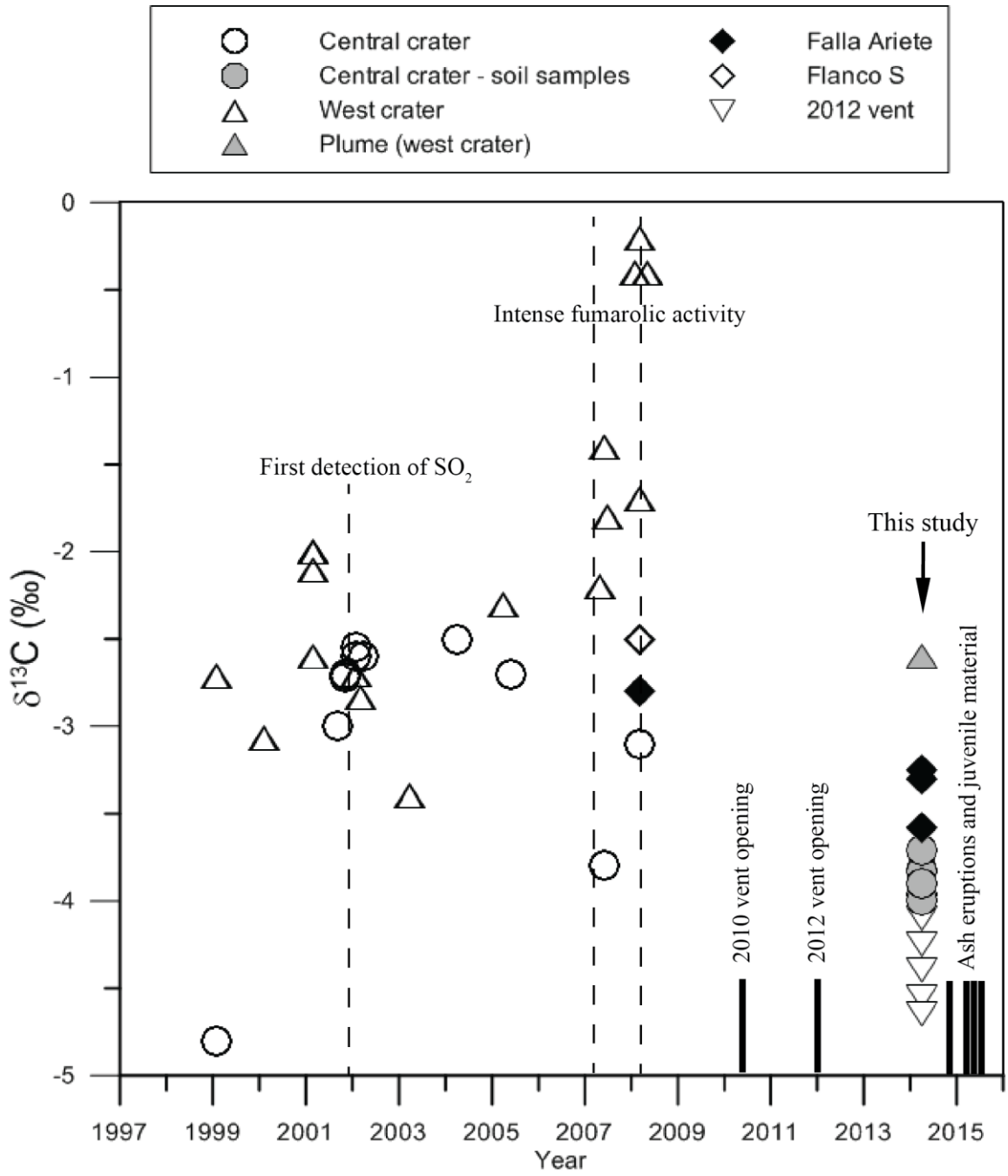

Figure 11: Carbon isotope measurements made on Turrialba since its reawakening in 1996 (Shaw et al. 2003; Vaselli et al. 2010; Hilton et al. 2010). The detection of SO_2 in late 2001 is the first indication of magmatic degassing (Vaselli et al., 2010). Vigorous fumarolic activity in the West crater from 2007-2008 results in very enriched $\delta^{13}C$ values (-0.2‰), while

Central crater values remain depleted (-3.3‰). Our measurements record the most depleted values since its reawakening, only 6 months prior to the onset of the eruptive period starting on October 31st, 2014.

The carbon isotopic record at Turrialba mainly illustrates the dominant influence of the hydrothermal system seen for the summit gases (Figure 11). From 1999-2008, Turrialba shows enrichment in the carbon isotopic composition of the fumarolic gases from both the Central and West craters, with values ranging from -2.0‰ to -3.5‰ and one value at -4.8‰ during the reawakening period. The hydrothermal system causes enrichment in ^{13}C during periods of intense fumarolic activity, producing isotopic values of up to -0.2‰ (Vaselli et al. 2010). This obscured the volcanic signature until the opening of the 2010 and 2012 vents permitted collection of high temperature gases. However, no carbon isotopic measurements have been made following the opening of the 2010 and 2012 vents until this study.

3.3 Methodology

3.3.1 Sample collection

This study combines field measurements with a Picarro G1101-i CRDS and laboratory measurements with an isotope ratio mass spectrometer (IRMS) to evaluate the CO_2 isotopic composition of Turrialba gases. Our measurements were made from April 1 – 6, 2014, during a period of active degassing preceding the first magmatic eruption on October 29th, 2014. Plume samples were collected from the western flank of Turrialba, on the rim and at the site of the permanent Multi-GAS station. Soil gas samples were collected at the Central crater fumaroles, near the 2012 vent and along the Falla Ariete, to serve as a comparison to the plume gases. The 2012 vent was sampled directly with the aid of a titanium tube, and fumaroles from Falla Ariete

were sampled with a soil gas probe. Ambient atmosphere measurements were made on the southern and eastern flanks of the volcano, away from regions impacted by volcanic gases. Locations are indicated in Figure 12.

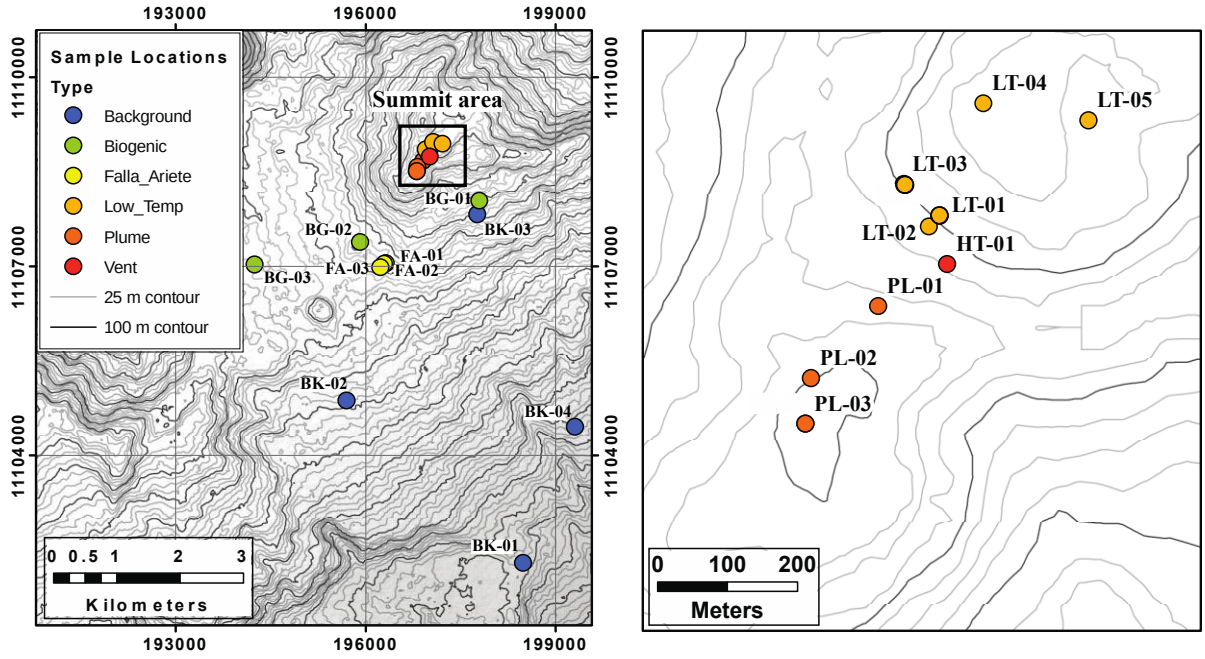

Figure 12: Sample locations at Turrialba volcano from April 1-6th 2014. Soil gas samples were taken at the Low temperature, Biogenic and Falla Ariete locations. Air samples were collected at the Vent, Plume and Background locations. All background samples were collected at locations unaffected by the volcanic plume, automobile combustion and crop burning. DEM source data: ASTER GDEM, a product of METI and NASA.

Gas samples were collected in duplicate, with at least one sample collected in a Tedlar gas bag for same-day analysis with the CRDS and another collected in a 30 mL evacuated vial

for laboratory analysis with the IRMS. The vials were evacuated to 150 mTorr and were pretreated with 0.2 μl of $HgCl_2$ to prevent bacterial respiration and isotopic fractionation during storage and transport. Both the plume and atmospheric samples were collected using a low flow pump built into an Crowcon CO_2 meter. The gas was pumped through several meters of Tygon tubing upwind of the pump to avoid capturing biogenic CO_2 from our respiration. The line was first purged with the sample by pumping gas for several minutes before samples were taken. Each Tedlar bag was also purged twice before being filled with approximately 1 L of gas for analysis. A 60 mL syringe was used to sample gas from the line while maintaining positive gas flow. A total of 50 mL of gas was injected into the 30 mL evacuated vial to create an overpressure. Soil gas samples were taken using a stainless steel probe coupled with the Crowcon pump or a hand pump to extract gas in the pore spaces, and were then sampled using bags and vials as described above.

Recent work has illustrated that the spectral lines of the G1101-i CRDS have an inherent interference with large (greater than ambient) quantities of H_2S (Malowany et al. 2015; Lucic et al. 2015). Turrialba has H_2S concentrations exceeding 20 ppm, which can cause large interferences with the CRDS. A simple metal scrub of copper was employed to eliminate H_2S from all samples prior to analysis, removing any potential interferent (Malowany et al. 2015). Thus, every sample collected from the plume or crater was passed through a 30 cm copper tube filled with copper filings to remove H_2S. The copper scrub was changed daily and monitored for visible signs of reaction by H_2S forming CuS.

3.3.2 Field-based isotopic measurements

The Picarro G1101-i CRDS for isotopic CO_2 was stationed ~5 km west of the summit at Turrialba Lodge (2650 m.a.s.l.), where there was a reliable power source to which we added an uninterruptible power supply in order to maintain a stable voltage for the instrument. The CRDS was operated continuously during sample analysis in the evenings at temperatures of 0 - 10° C and an average relative humidity of 65% in April. The G1101-i performs gas phase analysis for $^{12}CO_2$ (ppm), $^{13}CO_2$ (ppm), and $\delta^{13}C$ over a concentration range of 300-6,000 ppm CO_2 with a nominal precision of ± 0.85‰ (1σ) at 500 ppm (Lucic et al., 2015). The precision is concentration dependent and can vary by 0.6‰ over a concentration range of 500-5,000 ppm CO_2 (Lucic et al. 2015). To eliminate such variations, all samples and standards were diluted to 1000 ppm, except for the atmospheric and plume samples whose concentrations were generally less (400-1000 ppm). The soil gas samples had concentrations of 58 - 81% vol. CO_2 and needed to be diluted. To do this, we removed CO_2 from the ambient air using an ascarite (NaOH) scrub to produce CO_2-free air in the Tedlar bags with which to dilute high concentrations of CO_2.

We brought three in-house gas standards (-11.5‰, -16.0‰ and -43.0‰) to use for in-field instrument calibration. The standards have been analyzed against international standards using a Finnigan-MAT IRMS at the University of Toronto, and the CRDS is able to reproduce a 1:1 match on the standards with the Finnegan MAT (Figure 13). All gas samples collected during the day in the Tedlar gas bags were analyzed the same evening, for near real-time analysis. Each set of samples was bracketed with a set of standards at the beginning and end of analysis to monitor and correct for instrumental drift. Analysis time did not exceed 3 hours, and the instrumental drift during this period was negligible. Standards were reproduced within error each

day, indicating that daily results are comparable. This permitted a focused study of interesting areas on Turrialba, while also allowing us to resample areas after viewing the results.

The instrument was operated continuously during the evenings while samples were analyzed. The instrument measured ambient conditions in the lodge, which are variable (450 – 800 ppm CO_2) due to our respiration. For analysis, a sample bag was attached to the inlet, separated by a 1 μm Acrodisc CR 25 mm syringe filter to remove particulate matter, registering an increase or decrease in CO_2 and establishing a stable signal. The instrument used a flow-through system, taking one measurement every 10 seconds at a flow rate of 40 mL/ min. An individual gas bag (~1L) was analyzed for 15- 20 minutes, a period which produced sufficient measurements for statistical analysis. The statistical toolkit of the G1101-i was used to calculate the average $^{12}CO_2$ and $^{13}CO_2$ concentrations and the $\delta^{13}C$ value relative to Vienna Pee Dee Belemnite, which are reported here.

3.3.3 Laboratory analysis

The 30 mL evacuated vials containing 50 mL of sample were analyzed at the University of Toronto on a continuous flow Finnigan MAT gas source mass spectrometer with a Varian gas chromatograph for stable carbon. The reported precision for $\delta^{13}C$ is ±0.1‰, but lower concentration samples (<1000 ppm) had a higher reported uncertainty of up to ±0.5‰. Each sample was analyzed in duplicate and an in-house standard was analyzed every 10 samples to monitor instrument drift. Samples with high H_2S concentrations were sufficiently separated by the gas chromatograph so as to not interfere with the ^{12}C and ^{13}C peaks. There is excellent agreement between the CRDS measurements and the Finnigan MAT (Figure 13), except for a small deviation for the samples of the 2012 vent where the values differ by ~1‰. CO_2 and H_2S

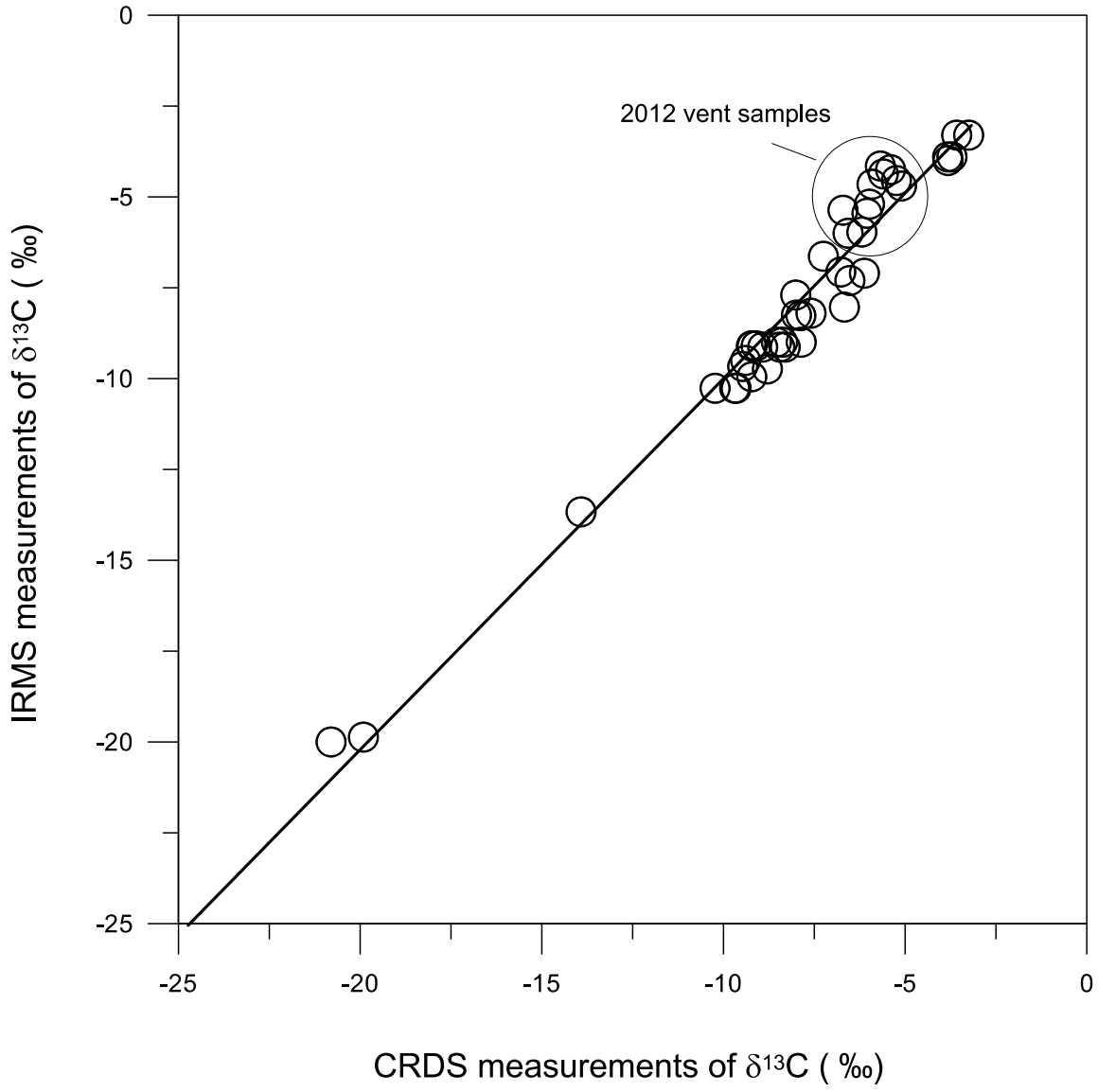

Figure 13: Comparison of $\delta^{13}C$ values from the Picarro G1101-i cavity ring-down spectrometer (CRDS) and the Finnegan MAT isotope ration mass spectrometer (IRMS). CRDS values of 2012 vent gases are slightly depleted with respect to the IRMS values, suggesting that the composition of the 2012 vent gases are causing a potential interference with the CRDS values. CRDS values for the plume measurements are within error, thus both data sets are used in the Keeling analysis.

concentrations were analyzed using gas chromatography. Large ranges in the CO_2 concentrations (380 – 88 000 ppm) generated results with concentration-dependent error. Two in-house standards were used for comparison, one with a concentration of 1996 ppm for the low concentration samples and one at 10 000 ppm for the high concentration samples. All samples were run in triplet, and the reported values include the mean and standard deviation for the three measurements. H_2S was only measured for the 2012 vent samples where we had observed an anomalous response from the CRDS. H_2S had previously been removed from all other samples using a copper tube as described above.

3.4 Results

3.4.1 Ambient atmosphere

Carbon isotope values are reported in Table 1 with associated CO_2 concentrations, H_2S concentrations and temperature measurements for each site. Reported isotopic compositions agree well with typical values for fumaroles, ambient atmosphere and biogenic soil gases. Concentrations of CO_2 in the ambient atmosphere averaged 405±26 ppm CO_2, slightly above the global average of 401.33 ppm (Scripps/NOAA, Mauna Loa CO_2; April, 2014, www.co2now.org). The background samples had $\delta^{13}C$ of -8.3‰ to -10.2‰, within the range of atmospheric values previously observed in rainforest environments (Keeling 1958; Lloyd et al. 1996; Trolier et al. 1996). Diurnal variations in the background CO_2 isotopic composition previously have been attributed to photosynthetic activities of plants, where the preferential

Table 1: CO_2 concentrations and isotope measurements using the cavity ring-down spectrometer (CRDS) and the isotope ratio mass spectrometer (IRMS). H_2S concentrations are included for samples with high concentrations. Reported error for the CRDS and IRMS measurements is ± 0.05‰ and 0.5‰, respectively.

Site ID	Easting NAD83	Northing NAD83	Altitude (m)	Date (dd/mm/yyyy)	Temp (°C)	CRDS Sample ID	CO_2 (ppm)[a]	$\delta^{13}C$ (‰)	IRMS sample ID	$\delta^{13}C$ (‰)	CO_2 (ppm)[b]	error (±ppm)	H_2S (ppb)	error (±ppb)
BG	**Biogenic**													
BG-01	197802	1108039	3015	01/04/2014		050414-S01	43498	-20.80	39-050414-S	-20.0	47346	3056		
BG-02	195914	1107384	2780	01/04/2014		050414-S02	8910	-21.04	38-050414-S		6837	645		
BG-03	194246	1107030	2657	01/04/2014		050414-S03	21538	-19.91	40-050414-S	-19.9	20443	132		
Average								**-20.58**		**-19.9**				
Stdev								**0.60**		**0.1**				
BK	**Background**													
BK-01	198493	1102292	1624	01/04/2014					01-010414-B	-9.8	449	16		
BK-01	198493	1102292	1624	06/04/2014		060414-B04	383	-8.45	42-060414-B	-9.1	424	1		
BK-01	198493	1102292	1624	06/04/2014		060414-B05	385	-8.30						
BK-01	198493	1102292	1624	06/04/2014		060414-B06	376	-8.92						
BK-02	195699	1104866	2435	01/04/2014					02-010414-B	-10.1	441	10		
BK-02	197769	1107825	2941	03/04/2014		030414-B01	391	-9.65	25-030414-B	-10.3	428	8		
BK-02	197769	1107825	2941	03/04/2014		030414-B02	389	-9.69						
BK-02	197769	1107825	2941	03/04/2014		030414-B03	399	-10.23						
BK-03	197769	1107825	2941	02/04/2014		020414-B01	418	-9.21	14-020414-B	-9.1	449	5		
BK-03	197769	1107825	2941	02/04/2014		020414-B02	410	-9.10						
BK-03	197769	1107825	2941	02/04/2014		020414-B03	407	-9.23						
BK-04	199312	1104454	1909	06/04/2014		060414-B01	371	-7.86	41-060414-B	-9.0	422	8		

BK-04	199312	1104454	1909	06/04/2014		060414-B02	374	-8.54						
BK-04	199312	1104454	1909	06/04/2014		060414-B03	373	-8.37						
Average								**-8.96**		**-9.6**				
Stdev								**0.69**		**0.5**				
FA	**Falla Ariete**													
FA-01	196320	1107047	2744	01/04/2014	89.9	060414-S02	701400	-3.58	44-060414-S	-3.3	694225	30970		
FA-01	196320	1107047	2744	01/04/2014	89.9	060414-S03	636270	-3.25	45-060414-S	-3.3	650070	13543		
FA-02	196295	1107036	2738	01/04/2014		060414-S01	746490	-5.98	43-060414-S	-5.2	794195	31330		
FA-03	196236	1106982	2726	01/04/2014		060414-S04	20603	-13.92	46-060414-S	-13.7	16680	1036		
HT	High Temperature (2012 vent)													
HT-01	197017	1108738	3200	04/05/2014	380.0	040414-F01	53739	-5.24	26-040414-F	-4.6	57420	1206	5962	240
HT-01	197017	1108738	3200	04/05/2014	380.0				27-040414-F	-4.4	65237	4254	5955	110
HT-01	197017	1108738	3200	04/05/2014	380.0				28-040414-F	-4.1	61734	140	5835	165
HT-01	197017	1108738	3200	04/05/2014	380.0	040414-F04	57162	-5.40	29-040414-F	-4.3	71303	2359	6325	128
HT-01	197017	1108738	3200	04/05/2014	380.0	040414-F05	63000	-5.91	30-040414-F	-4.7	49573	1117	6698	535
HT-01	197017	1108738	3200	05/04/2014	480.0	050414-F01	126072	-5.60	34-050414-F	-4.4	75791	2147	7390	370
HT-01	197017	1108738	3200	05/04/2014	480.0	050414-F02	101606	-5.10	35-050414-F	-4.7	78211	1161	5531	168
HT-01	197017	1108738	3200	05/04/2014	480.0	050414-F03	97667	-5.68	36-050414-F	-4.2	97662	2374	7138	584
HT-01	197017	1108738	3200	05/04/2014	480.0	050414-F04	109383	-5.16	37-050414-F		86511	256		
HT-01	197017	1108738	3200	05/04/2014	480.0	050414-F05	98273	-5.67						
Average								**-5.47**		**-4.4**				
Stdev								**0.29**		**0.2**				
LT	**Low Temperature**													
LT-01	197006	1108808	3176	04/04/2014	87.9	040414-S01	768033	-3.96						
LT-02	196991	1108792	3185	04/04/2014	90.0	040414-S02	741480	-4.91						

LT-03	196955	1108853	3187	04/04/2014	88.0	040414-S03	584667	-3.82	31-040414-S	-4.0	680442	34679
LT-04	197069	1108968	3150	04/04/2014	73.6	040414-S04	629256	-3.83	32-040414-S	-3.9	686062	2751
LT-05	197219	1108944	3153	04/04/2014	76.5	040414-S05	772041	-3.71	33-040414-S	-3.9	809916	814
Average								**-4.05**		**-3.9**		
Stdev								**0.49**		**0.1**		
PL	**Plume**											
PL-01	196918	1108678	3240	02/04/2014		020414-P06	530	-7.87	09-020414-P	-8.3	553	51
PL-01	196918	1108678	3240	02/04/2014		020414-P07	528	-7.59	10-020414-P	-8.2	527	13
PL-01	196918	1108678	3240	02/04/2014		020414-P08	481	-8.27				
PL-01	196918	1108678	3240	02/04/2014		020414-P09	506	-7.99	12-020414-P	-8.3	504	2
PL-01	196918	1108678	3240	02/04/2014		020414-P10	489	-8.01	13-020414-P	-7.7	519	1
PL-02	196822	1108575	3275	03/04/2014		030414-P01	751	-6.57	15-030414-P	-6.0	775	19
PL-02	196822	1108575	3275	03/04/2014		030414-P02	871	-6.19	16-030414-P	-6.0	873	5
PL-02	196822	1108575	3275	03/04/2014		030414-P03	867	-6.38	17-030414-P	-5.2	1044	7
PL-02	196822	1108575	3275	03/04/2014		030414-P04	970	-6.05	18-030414-P	-5.5	968	7
PL-02	196822	1108575	3275	03/04/2014		030414-P05	845	-6.71	19-030414-P	-5.4	1082	72
PL-03	196814	1108510	3281	02/04/2014		020414-P01	620	-6.77	04-020414-P	-7.1	689	6
PL-03	196814	1108510	3281	02/04/2014		020414-P02	714	-6.52	05-020414-P	-7.3	676	17
PL-03	196814	1108510	3281	02/04/2014		020414-P03	716	-6.12	06-020414-P	-7.1	703	12
PL-03	196814	1108510	3281	02/04/2014		020414-P04	647	-6.67	07-020414-P	-8.0	584	11
PL-03	196814	1108510	3281	02/04/2014		020414-P05	566	-7.25	08-020414-P	-6.6	685	122
PL-03	196814	1108510	3281	03/04/2014		030414-P06	473	-8.79	20-030414-P	-9.7	471	72
PL-03	196814	1108510	3281	03/04/2014		030414-P07	441	-9.22	21-030414-P	-10.0	437	3
PL-03	196814	1108510	3281	03/04/2014		030414-P08	438	-9.20				
PL-03	196814	1108510	3281	03/04/2014		030414-P09	426	-9.47	23-030414-P	-9.7	449	8
PL-03	196814	1108510	3281	03/04/2014		030414-P10	432	-9.39	24-030414-P	-9.5	446	14
PL-03	196814	1108510	3281	03/04/2014		030414-P11	425	-9.23				

PL-03	196814	1108510	3281	03/04/2014		030414-P12	436	-9.09	
Average								**-7.70**	**-7.5**
Stdev								**1.23**	**1.6**

[a] CO_2 concentrations measured by the CRDS

[b] CO_2 concentrations measured by gas chromatography (GC)

uptake of ^{12}C results in a peak ambient $\delta^{13}C$ value at mid-day and a corresponding CO_2 minimum (i.e. Lloyd et al. 1996). Our measurements were made following this mid-day isotopic maximum; as a result, we observed slightly more negative background values from samples taken later during the day (-9.7‰ to -10.2‰), compared to those taken near midday (-7.8‰ to -8.5‰). Figure 14 illustrates the observed decrease in $\delta^{13}C$ values from noon to late afternoon, resulting from an increase in the cellular respiration of plants and a decline in photosynthetic activity following the mid-day $\delta^{13}C$ maximum. To determine the appropriate atmospheric composition to compare with the plume compositions for our mixing calculations, we averaged background values taken during early afternoon (-9.2 ± 0.1‰), the period during which the plume samples were also collected.

3.4.2 2012 vent

The limited accessibility and very high temperature of the 2012 vent made sample collection challenging at this locality. Gases were sampled using a titanium tube as they emerged from the vent. We have assumed limited mixing with the ambient air due to the high concentrations (> 5% vol. CO_2) and elevated temperatures of the emerging gas. Temperature readings using a thermocouple indicated temperatures of between 380°C and 480°C for the measured gases; actual temperatures could be higher. Initial results from the CRDS showed little variability and a reported CO_2 isotopic composition of -5.5‰ ± 0.3‰. By contrast, IRMS measurements returned isotopic values of -4.4‰ ± 0.2‰ for the 2012 vent gases, suggesting that there is a ~1.1‰ discrepancy between the two types of measurements. Interference resulting from large variations in the noble gas composition of these high temperature gases potentially can cause a bias for the CRDS measurements (Nara et al. 2012). Since this site was the only

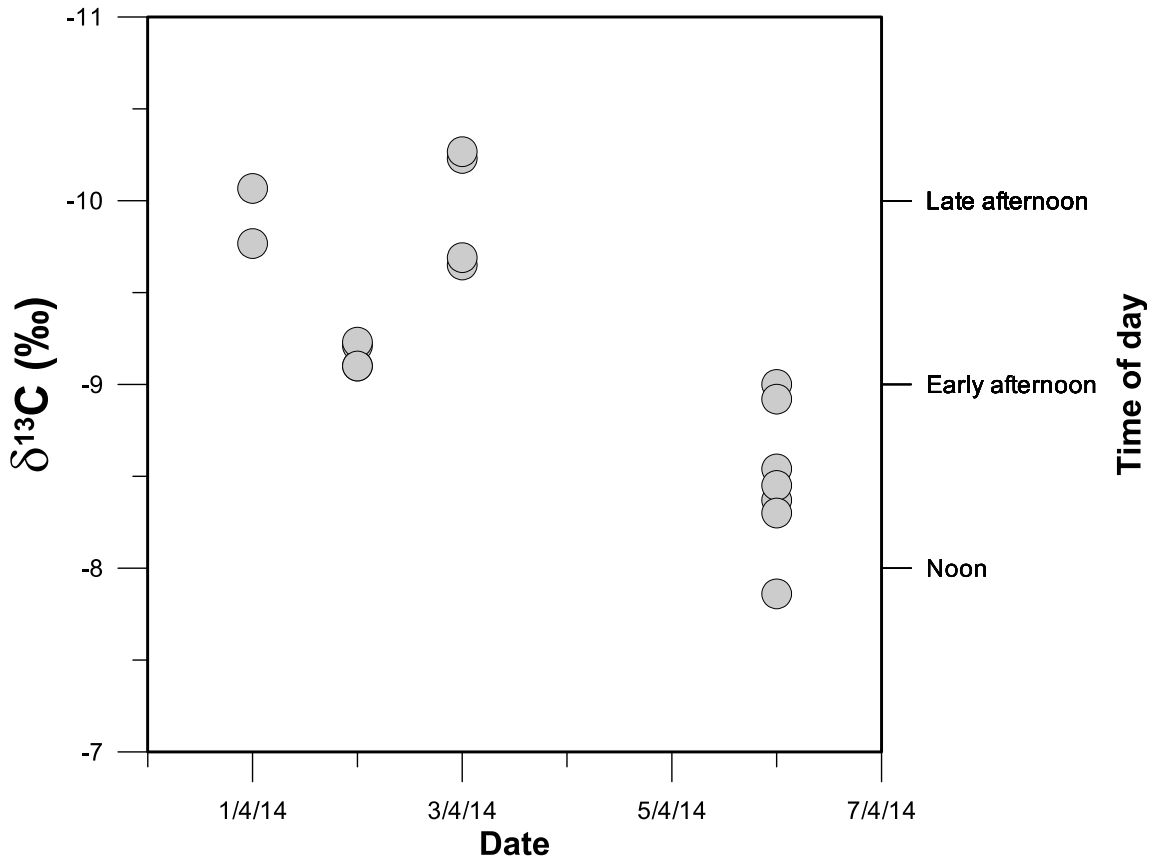

Figure 14: Variations in ambient atmosphere $\delta^{13}C$ values illustrate a temporal change resulting from photosynthetic activity. Plant respiration maintains an atmospheric composition close to -10‰, but, photosynthetic activity during daylight hours enriches the isotope values. This can cause diurnal variations in the $\delta^{13}C$ signature in regions with abundant vegetation (i.e., rainforest environments). At Turrialba we observe a diurnal range of ~2‰, with a maximum occurring near midday (-8.6‰ avg. value BK-04). We have used late afternoon values (-9.6‰ avg. of BK-02 and BK-03) to compare with the volcanic plume because they reflect the atmospheric composition at the time that the plume samples were taken.

location where IRMS and CRDS values varied by more than the reported errors of the IRMS (0.5‰), it is reasonable to assume that the variations in background noble gas chemistry may have caused a small shift in our CRDS values.

Relative to $\delta^{13}C$ measurements previously reported for fumaroles at Turrialba volcano, the 2012 vent samples are the most depleted $\delta^{13}C$ measurements reported since its reactivation in the mid-late 1990's (Figure 11). CO_2 gas with an average $\delta^{13}C$ value of -4.4‰ suggests the presence of a partially degassed magma and reflects a melt isotopic compositions of -8.4‰, assuming a fractionation factor of +4.00‰ between the gas and the melt phase at temperatures > 600°C (Javoy et al. 1986; Javoy et al. 1978). An undegassed basalt has a $\delta^{13}C$ signature of -6.5‰ ±1.5‰ (Javoy et al. 1986), which is more enriched than the inferred isotopic composition of the magma at Turrialba, suggesting that the magma is at least partially degassed.

3.4.3 Soil gases

Low temperature soil gas samples from the central crater had a range of -3.7‰ to -4.9‰ and an average value of -4.0‰ ± 0.4‰. The soil samples show a spatial correlation with distance from the 2012 vent and (Figure 15). Gases sampled close to the 2012 vent had higher temperatures and were more depleted in the heavy isotope, approaching the composition of the 2012 vent (-4.4‰). For example, sample LT-01 was closest to the 2012 vent (62 m) and had the most depleted isotopic values measured (-4.91‰). By contrast, soil gases at a distance of 294 m from the 2012 vent (sample LT-05) exhibited $\delta^{13}C$ of -3.7‰.

A series of soil gas samples were taken along the Falla Ariete, approximately 1 km outside the central crater. At this location, the fault is expressed as a gulley ~50 m wide. Soil gases were sampled near fumaroles along the east side of the gulley (FA-01) and have a narrow

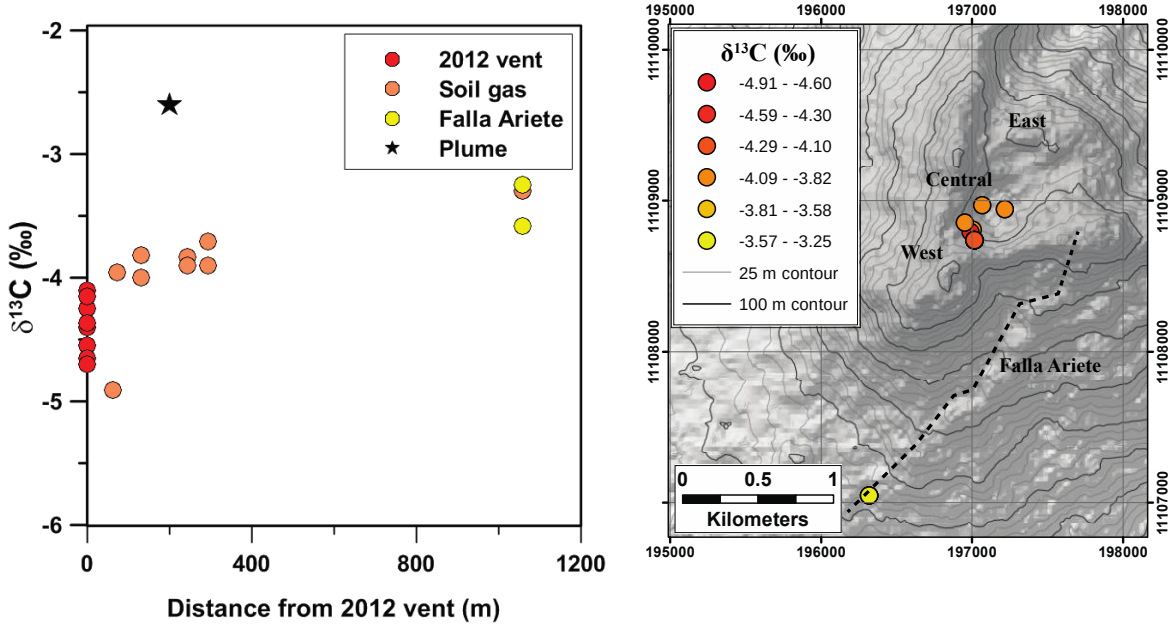

Figure 15: Increase in the measured isotope values with increasing distance from the 2012 vent. The extrapolated plume composition portrays values significantly more enriched in ^{13}C than those from either the 2012 vent or the soil gases. Gases emitted along the Falla Ariete regional fault system are likely derived from the local hydrothermal system and represent a hydrothermal endmember for gases at Turrialba volcano. DEM source data: ASTER GDEM, a product of METI and NASA.

isotopic composition of -3.4‰ ± 0.1‰. Sample FA-02 was taken at the base of the gulley, where there was evidence of tree kill from extremely high CO_2 concentrations (>79% vol. CO_2), but no visible degassing. The isotopic composition of this sample was slightly depleted (-5.6‰) compared to those from the nearby fumaroles. Vegetation present on the gulley floor may be contributing to the negative values at this location relative to the soil samples at FA-01. For comparison with FA-02, a soil gas sample was taken outside the gully on the west side of the

fault (FA-03); this sample had a $\delta^{13}C$ of -13.8‰, suggesting a mixture between magmatic and biogenic CO_2. On the flank of the volcano where there was no evidence of volcanic gases being emitted, soil gas samples BG-01, BG-02, and BG-03 have an average value of -20.3‰ ± 0.6‰, representative of the typical isotopic composition of organic soil in equatorial climates, which is a mixture of respired CO_2 from C3 and C4 plants (Cerling and Quade 1993; Cerling 1984).

3.4.4 Volcanic plume

The only real-time measurements of $\delta^{13}C$ in a volcanic plume to date have been made recently on Etna volcano using an isotope ratio infrared spectrometer (Rizzo et al. 2014). Hence, this is the second attempt at using portable instruments to analyze the isotopic character of a volcanic plume. The plume at Turrialba is composed mainly of gases from the West crater, where vigorous fumarolic activity generates a large proportion of the plume gases. At sampling locations P-01, P-02 and P-03, we collected a range of samples whose concentrations decreased from 1036 ppm to 435 ppm CO_2 with increasing distance from the fumaroles. Plume samples at near atmospheric concentrations (e.g. PL-01 and PL-03) range in isotopic composition from –6.6 to -10.0‰, whereas higher plume CO_2 concentrations (> 750 ppm) taken at PL-02 had more enriched isotopic signatures (-6.0‰ to -5.2‰). The plume samples represent mixing between atmospheric and magmatic endmembers. In Figure 16, the regression line defined by the plume samples illustrates this mixing trend between the magmatic and atmospheric compositions. Since the magmatic endmember has a much greater CO_2 concentration, the y-intercept of this 'Keeling-type' plot (Keeling, 1958) represents the isotopic composition of the pure magmatic endmember. The standard least squares regression (LSR) method is used for the Keeling plot (Zobitz et al. 2006), and it predicts a magmatic carbon isotope composition of -2.6 ±1.4‰, where the standard

error of the y-variable is computed according to Taylor (1998). The less common orthogonal distance regression (ORD) method (Model 2 Regression) recommended by Pataki et al. (2003) results in a predicted isotopic composition of -3.1 ±1.4‰. Both methods give similar results, but the orthogonal distance method introduces a negatively skewed bias in the predicted y-intercept, which arises from somewhat greater variability in the dependent variable than the independent variable for a linear regression (Zobitz et al. 2006). For our analysis, we apply the least squares approach and report the average composition of the magmatic endmember represented by the volcanic fumaroles in the West crater to be -2.6±1.4‰.

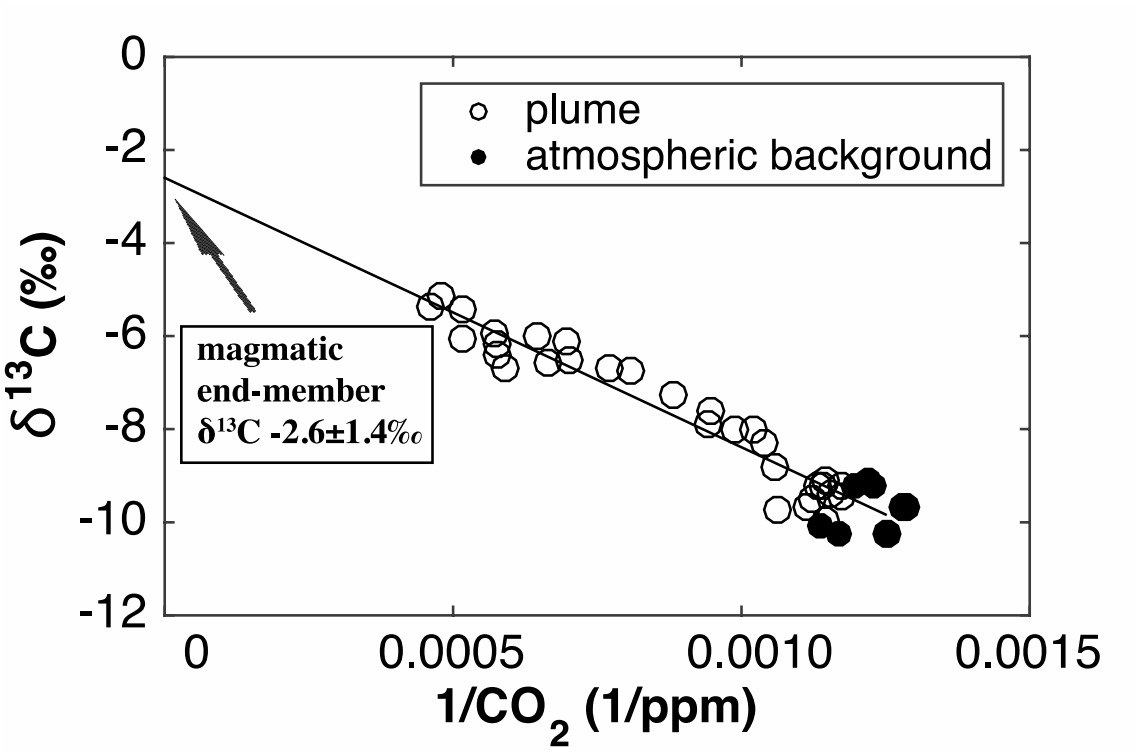

Figure 16: Keeling plot of the plume gas from Turrialba volcano, illustrating a mixture between the high concentration magmatic source and the ambient atmosphere (background). A least squares regression (LSR) predicts a magmatic source composition of -2.6±1.4‰.

3.5 Discussion

3.5.1 The Keeling method

This is the first attempt to apply the Keeling approach to a volcanic plume, and it has some key advantages. This method is a fast and accurate way to predict the magmatic source composition and is easily adaptable to small and large datasets without requiring large computational power, such as necessitated by the Monte Carlo method (Chiodini et al. 2011). However, we must consider the statistical methods applied to the Keeling plot and be aware of the changes in the environmental conditions that can influence the predicted isotopic values. We observed that the regression type (least squares regression vs. orthogonal distance regression) has a small bearing on the resulting isotope value predicted for the magmatic source. We reported the isotopic values from both techniques, which differed from each other by 0.5‰. The least squares regression (LSR) is more appropriately applied to the Keeling plot because it treats $\delta^{13}C$ and the CO_2 concentration as co-dependent variables (Zorbitz et al. 2006). The orthogonal distance regression (ODR) treats $\delta^{13}C$ and CO_2 concentration as independent variables, which results in a overweighting of the y-values. This is manifested as slightly depleted isotopic values predicted by the ODR method as compared to the LSR method. We recommend that all future use of the Keeling plot apply a least squares regression.

Daily variations in the atmospheric $\delta^{13}C$ composition make comparison of plume measurements taken at different times of day challenging. Diurnal variations in photosynthesis and plant respiration can cause relatively large isotopic variations in the background compositions of up to 2‰ in areas where vegetation is abundant. The magnitude of these isotopic variations is dependent upon the degree of biogenic influence in a particular region

(Lloyd et al. 1996; Keeling 1958); therefore, we anticipate that these fluctuations should be greater in rainforest areas (e.g., Costa Rica) and negligible in semi-arid or desert regions. The daily variations in background composition affect the plume compositions throughout the day, generating depleted values in the mornings and evenings, and enriched compositions at noon when photosynthesis is most efficient. When collecting repeated plume measurements, it is important to take them at the same time of day to best compare them. This is especially important for low concentration within 200 ppm of the background atmospheric concentration. Our plume measurements were taken daily between 13:00 and 15:00 local time, when background compositions were ~9 ‰. This allows measurements from multiple days to be compared with confidence. The plume compositions were collected over a large range in CO_2 concentration (400-1000 ppm CO_2), which minimizes effects from small variations in background composition during this time. Monitoring the changes in isotopic composition of the magmatic source using plume measurements is a promising tool for volcano monitoring; however, in regions with dense vegetation, a careful background characterization should be conducted before plume measurements are compared on a daily basis.

3.5.2 Spatial and temporal variations of carbon isotopes at Turrialba

Using the Keeling approach and an ordinary least squares regression (Zobitz et al. 2006), we predict a composition of -2.6±1.4‰ for the source of the volcanic plume. Since the plume is dominantly sourced from the West crater, we assume that this value is representative of the composition of the west crater fumaroles. This isotopic signature is more enriched in ^{13}C than the soil gases from the central crater (-3.4‰) and those from the 2012 vent (-4.4‰). Combined, the isotope values from these three sources reveal heterogeneity in the volcanic CO_2 composition at

Turrialba volcano. Previous studies have also recognized variations in the isotopic composition of CO_2 at Turrialba (Hilton et al. 2010; Shaw et al. 2003; Vaselli et al. 2010). Evidently, these variations have persisted over time and have become more pronounced.

One explanation for this spatial variation is the 'drying out' of the hydrothermal system (Moussallam et al. 2014), resulting in $\delta^{13}C$ variability between magmatic and hydrothermal signals. During the period of 2001-2007 the carbon isotope compositions did not show much variability due to the presence of a shallow hydrothermal system which buffered carbon isotopes to values between -2.0‰ and -3.5‰ (Figure 11; Martini et al. 2010; Vaselli et al. 2010; Shaw et al. 2003). Vogel et al. (1970) illustrated experimentally that exchange of carbon between the liquid and gas phase can produce a temperature-dependent fractionation, where ^{13}C prefers the gas phase. This could explain the enriched isotope values from fumaroles and soil gases that are fed by the hydrothermal system. In 2007, the 'magmatic phase' commenced, marked by a sharp increase in fumarolic output exceeding the capacities of a hydrothermal system (Martini et al. 2010). During this period, several medium temperatures fumaroles (~200°C) in the West crater had isotopic values reaching -0.2‰ under supercritical conditions (Vaselli et al. 2010). The liquid-gas fractionation of carbon isotopes at temperatures >120°C has not been determined experimentally, but low temperature experiments suggest that the fractionation of carbon isotopes is greater at higher temperature (Vogel et al. 1970; Mook et al. 1974). This would help explain the observed increase in $\delta^{13}C$ to -0.2‰, during periods when the fumarole temperatures exceeded 200°C. Following the opening of the 2010 and 2012 vents on Turrialba, Moussallam et al. (2014) noted a distinct contrast between the CO_2/SO_2 ratio of the plume (2.59) and the 2010 vent (1.76). This chemical contrast is the first sign of a truly heterogeneous signal from Turrialba. Their results suggest that a magmatic signal was derived from the high temperature

vents (i.e., the 2010 and 2012 vents) and a hydrothermal signal from the fumaroles in the West crater. We propose that the hydrothermal system buffers the CO_2/SO_2 ratio and the $\delta^{13}C$ composition of the fumarolic and soil gases, while the 2012 vent is producing a more magmatic signal, which is unmodified by hydrothermal interaction.

Assuming that the observed heterogeneity in carbon isotopes is a product of hydrothermal buffering of a magmatic fluid in which the 2012 vent represents the deep degassing magmatic endmember, we would expect to see a distribution in isotopic values which are more magmatic near the 2012 vent and more hydrothermal with increasing distance from the source region. Soil gases collected from the Central crater appear to show this trend as they decrease in temperature and increase in $\delta^{13}C$ with increasing distance from the 2012 vent (Figure 15). LT-02, the sample closest to the 2012 vent, has a $\delta^{13}C$ of -4.9‰. This value is within the range of those observed from the 2012 vent, and it is also very close to the site of the first major eruption of the volcano on October 29st, 2014. Therefore, it is attributed to have a dominantly magmatic value. Conversely, the Falla Ariete soil gases (FA-01) are the furthest from the 2012 vent, and have the most enriched $\delta^{13}C$ composition at -3.3‰, similar to the values in the West crater during the hydrothermal-magmatic stage from 2001-2007 (Vaselli et al. 2010; Hilton et al. 2010; Shaw et al. 2003). The Falla Ariete is 1 km distant from the summit; dissolved gas is likely transported there via a hydrothermal system that exploits the fault's permeability.

Hilton et al. (2010) attributed temporal variations in the $\delta^{13}C$ composition at Turrialba to changes in the source contribution from the subducting slab using helium and carbon isotopes. This approach assumed negligible hydrothermal alteration due to the relatively small variation in fumarole temperature. In March 2001, a sharp decrease in $CO_2/^3He$ and corresponding increase in $\delta^{13}C$ from –4.1‰ to -3.8‰ illustrates an increase in the mantle-derived component during this

time (Hilton et al. 2010); this is coincident with the onset of the hydrothermal-magmatic phase (Martini et al. 2010). However, if the hydrothermal system is altering the magmatic $\delta^{13}C$ value, then these estimates will additionally show changes that do not necessarily reflect the changes in the proportions of slab and mantle inputs. Duplicate measurements from this study reveal heterogeneity in $\delta^{13}C$ in March 2001 where measured values were -4.4‰ and -3.8‰. The $\delta^{13}C$ value of -3.8‰ was selected for their calculations on the basis that it had the least air contamination. However, the reported $^{4}He/Ne$ of both samples suggests that they both have negligible air contamination. Instead, the shallow hydrothermal system may be buffering $\delta^{13}C$ to higher values, similar to those we observed in our crater soil gas samples. We propose that the isotopic signatures observed by Hilton et al. (2010) and Shaw et al. (2003) also demonstrate heterogeneity in the CO_2 composition at Turrialba. Their results indicate that temporal variations in the isotopic composition of the fumarolic gases are due solely to variations in the slab input; however, we suggest that the shallow hydrothermal system may also be influencing the isotopic character.

Hydrothermal systems appear to influence the isotope composition of CO_2 substantially. Separation of CO_2 between gaseous and aqueous phases can enrich gaseous CO_2 in ^{13}C with respect to the dissolved CO_2 (Vogel et al. 1970). The fractionation factor between the dissolved CO_2 and gaseous CO_2 increases with temperature, causing larger variations. If the hydrothermal system at Turrialba is releasing dominantly non-aqueous CO_2, the enrichment of the soil gas and plume signatures may be a result of isotope partitioning between gas and water. The hydrothermal overprint makes it challenging to use fumarole and soil samples to constrain the magmatic endmember. The opening of the 2010 and 2012 vents have provided an opportunity to

better estimate the magmatic gas composition where the hydrothermal system has minimal impact.

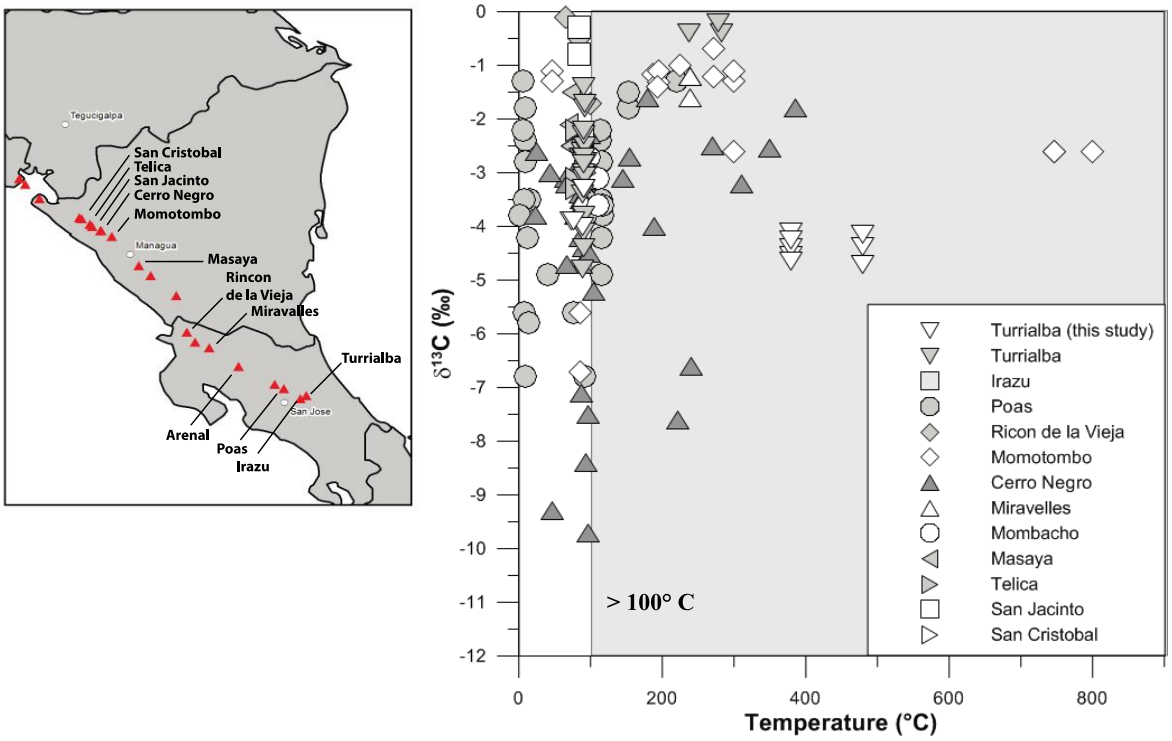

Figure 17: CO_2 isotope composition of gases from active volcanoes in Costa Rica and Nicaragua. Large range in observed values at low temperatures. High temperature samples are less common and generally show a narrower range of compositions. Overall, Turrialba has a more depleted $\delta^{13}C$ signature compared to the rest of the arc. Data compiled from Snyder et al. 2001; Shaw et al. 2003; Sano and Williams 1996; Vaselli et al. 2010; Hilton et al. 2010; Fischer et al. 2015; Lucic et al. 2014; Allard 1983; Tassi et al. 2004.

3.5.3 Implications for magma degassing at Turrialba

Continued eruptive activity at Turrialba from 29 October 2014 to the time of writing indicates that dominantly magmatic gases are currently being released from a degassing magma

body. Detection of magmatic volatiles in 2007 (Vaselli et al. 2010) was the first indication of new magma below Turrialba, but it remains undetermined whether a new magma input is responsible for the recent eruptive period, or if melt remobilization was initiated at the beginning of its re-awakening. Carbon isotopic studies allow us to track the magmatic signature of degassing magma (Gerlach and Taylor, 1990; Taylor, 1986). The isotopic signature of the most magmatic gases (-4.4‰) from this study is consistent with a slightly degassed magma body below Turrialba. The long period of degassing that preceded the recent eruptions suggest that a magma injection initiated activity at Turrialba as early as 1996, with open vent degassing persisting for the next 18 years. It is likely that magma has been present below Turrialba since 1996 and that either continual replenishment from a deep source or melt remobilization of crystallizing mush have provided the continual supply of volatiles during this period of active degassing. A persistent body of magma helps to explain the degassed signature observed in the carbon isotopic signature. Alternatively, we are witnessing an isotopic composition that is characteristic of the undegassed magmatic signature at Turrialba. Studies of carbon isotopes at other volcanoes from the Central American Volcanic Arc (CAVA) indicate that the $\delta^{13}C$ values observed at Turrialba are slightly more depleted in ^{13}C (Figure 17). Most isotopic measurements along the CAVA have been made from low temperature fumaroles, with only a few which are >100°C (Figure 17). If the isotopic composition from the 2012 vent is representative of an un-degassed magma, contributions of carbonate-rich fluids from the subducting slab beneath Turrialba may be enriching volcanic CO_2 in ^{12}C relative to other volcanoes in the Central American Volcanic Arc. However, the persistence of magmatic volatiles at Turrialba since 2007 indicates that a new magma body has been present beneath Turrialba for almost a decade, and potentially since its reawakening in 1996. Further study of the long-term isotopic character of

Turrialba will reveal a consistent model for its degassing behavior and melt composition. The isotopic compositions of magmatic gases reported in this study support the presence of a degassing magma body beneath Turrialba since the late 1990's. Variations in $\delta^{13}C$ observed since 1996 suggest that a hydrothermal system has transported magmatic volatiles to the surface and buffered the CO_2 isotopic composition. The low temperatures of the measured fumaroles (<200° C) is consistent with transport by a hydrothermal system until the opening of the 2010 and 2012 vents provided direct conduits for magmatic volatiles to the surface by sourcing high temperature gases.

3.6 Conclusions

Portable cavity-enhanced absorption spectrometers allow field analysis of isotopic compositions, enabling assessment of the data in near real-time. We used a portable cavity ring-down spectrometer (CRDS) to evaluate the isotope composition of CO_2 gas at Turrialba volcano in April 2014. Fortuitously, this was 6 months prior to Turrialba's first major eruption since its re-awakening in 1996. Carbon isotope measurements from the high temperature vent reveal a stable isotope composition of -4.4±0.1‰ for the magmatic source. Isotope values extrapolated from the volcanic plume using the Keeling method are significantly more enriched in their isotope composition (-2.6‰). The source of the volcanic plume is derived from fumaroles dominated by hydrothermal activity. Soil gas samples from the central crater and a regional fault system (Falla Ariete) reveal heterogeneity in the isotopic signature, with $\delta^{13}C$ values becoming more enriched further from the 2012 vent (-4.9‰ to -3.3‰). Modification of the magmatic carbon isotopic signature by the local hydrothermal system may explain the heterogeneous signal observed at Turrialba. It is important to characterize the magmatic value at Turrialba through

continued monitoring of $\delta^{13}C$, especially for the high temperature vents. Only then can comparisons be made to link changes in carbon isotope composition to degassing behaviour or changes in the carbon source composition.

Chapter Four: Major conclusions and suggestions for future work

The most salient points of this thesis are as follows:

1. In order to use the CRDS on volcanoes, interferences arising from anomalous gas concentrations must be removed. Hydrogen sulfide gas produces a significant negative interference upon $\delta^{13}C$ of the G1101-i CRDS resulting from spectral interference with the ^{12}C and ^{13}C lines in the near infrared region of the electromagnetic spectrum. This interference is linear and dependent on the CO_2 and H_2S concentrations of the sample. Future work with the G1101-i CRDS and other CRDS instruments that operate in the near infrared should employ a metal scrub (i.e., copper, lead, zinc) to remove H_2S from the gas sample before it is analysed by the CRDS. These scrubs do not modify the $\delta^{13}C$ and are easily monitored for efficiency.

2. Fluctuations in the background atmospheric $\delta^{13}C$ composition are pronounced in highly vegetated areas. Near Turrialba volcano, the rainforest produces a 2‰ variation between the early morning and late afternoon. It is advisable to take plume measurements at a single time of day for inter-comparison of measurements, thus avoiding variations associated with biogenic respiration and photosynthesis.

3. The Keeling method is an effective approach for predicting the isotopic signature of the volcanic source using a least squares regression. The plume composition from Turrialba is dominated by fumaroles in the West crater having an isotopic value of -2.6‰. This differs substantially from the measured composition of the 2012 vent (-4.4‰), showing heterogeneity in the isotopic signature between the high temperature vent and the

fumarole-dominated plume. Future monitoring campaigns should situate plume measurements near high temperature vents to capture the most magmatic signature.

4. The local hydrothermal system on Turrialba is modifying the carbon isotopic composition of CO_2 such that soil gas $\delta^{13}C$ compositions are more enriched in ^{13}C with increasing distance from the 2012 vent. The hydrothermal system is the primary conduit for magmatic volatiles to the surface; however, the isotopic signature of the magmatic gases is being modified by gas-liquid separation of CO_2.

5. This work presents the first $\delta^{13}C$ measurements since the opening of the 2010 and 2012 vents which source deep magmatic gas. Their isotopic composition is among the most depleted observed on Turrialba and is consistent with a partially degassed melt sourcing volatiles. Progressive drying-out of the hydrothermal system will present further opportunities for measurements of the unmodified volcanic gas, and continual monitoring of the vent gases may provide new insight for degassing trends and magma replenishment.

Isotopic studies provide valuable information on magmatic systems and their interaction with the environment. Examination of carbon isotopes with portable cavity ring-down spectrometers is allowing for a wider application of isotopic studies in volcanic systems. In the future, CRDS will facilitate larger temporal and spatial studies that previously have been difficult using traditional mass spectrometry. This works presents a spatial study of carbon isotopes conducted over the period of one week. If deployed for longer periods, these instruments will provide valuable real-time feedback on spatial heterogeneity and temporal

variations in isotopic composition. Currently, isotopic measurements are rarely implemented as monitoring tools on active volcanoes due to the lag time between field sampling and laboratory analysis. The CRDS can be deployed in the field and make measurements in near-real time or even real-time, providing data acquisition and analysis in a timely manner for monitoring. A long-term study of volcanic activity and evolution of $\delta^{13}C$ is the next step for applying these instruments as forecasting tools.

Cavity ring-down spectrometers also have the ability to make isotopic measurements of small molecules (e.g., CO_2, H_2O, CH_4, N_2O, etc.). At the time of writing, only isotopic measurements of CO_2 have been made with the CRDS on active volcanoes. Adapting CRDS for isotopic H_2O, and CH_4 on active volcanoes will aid in developing a suite of isotopic tools for the study of volcanic gases.

This work and previous studies have resolved many of the interferences that may arise with the CRDS (e.g., H_2S. H_2O, CH_4). Comparison of CRDS measurements with IRMS measurements of gases from Turrialba volcano were in excellent agreement, except for samples from the 2012 vent where the values differed by 1‰. In this case, the IRMS values were used for data analysis, and future work should be done to identify the sources of interference from high temperature vent gases.

A major conduit for magmatic volatiles to the surface is through local hydrothermal systems. Interaction of CO_2 in a hydrothermal system can modify the magmatic $\delta^{13}C$ signature through processes of liquid-gas phase interaction (Vogel et al. 1970) and temperature-dependent calcite dissolution or precipitation (Emrich et al. 1970). When applying small isotopic differences (i.e. 1-2‰) to differentiate degassing trends or compositional differences in the melt source, isotopic overprinting resulting from

hydrothermal alteration can significantly affect the results. At Turrialba, there is strong evidence for hydrothermal modification of $\delta^{13}C$, and further work should be conducted to understand this hydrothermal control.

References

Aiuppa, A., P. Robidoux, G. Tamburello, V. Conde, B. Galle, G. Avard, E. Bagnato, J. M. De Moor, M. Martínez, and A. Muñóz. 2014. "Gas Measurements from the Costa Rica–Nicaragua Volcanic Segment Suggest Possible along-Arc Variations in Volcanic Gas Chemistry." *Earth and Planetary Science Letters* 407 (December): 134–47. doi:10.1016/j.epsl.2014.09.041.

Allard, P. 1983. "The Origin of Hydrogen, Carbon, Sulphur, Nitrogen and Rare Gases in Volcanic Exhalations: Evidence from Isotope Geochemistry." *Forecasting Volcanic Events* 1: 337–86.

Barboza, V., E. Fernàndez, E. Duarte, W. Sáenz, M. Martínez, N. Moreno, T. Marino, et al. 2003. "Changes in the Activity of Turrialba Volcano: Seismicity, Geochemistry and Deformation." *Seismol Res Lett* 74: 215.

Burton, M. R., G. M. Sawyer, and D. Granieri. 2013. "Deep Carbon Emissions from Volcanoes." *Reviews in Mineralogy and Geochemistry* 75 (1): 323–54. doi:10.2138/rmg.2013.75.11.

Carapezza, M. L., Inguaggiato, S., Brusca, L. and Longo, M.: Geochemical precursors of the activity of an open-conduit volcano: The Stromboli 2002–2003 eruptive events, Geophys. Res. Lett., 31(7), L07620, doi:10.1029/2004GL019614, 2004.

Carr, M. J., M. D. Feigenson, and E. A. Bennett. 1990. "Incompatible Element and Isotopic Evidence for Tectonic Control of Source Mixing and Melt Extraction along the Central American Arc." *Contributions to Mineralogy and Petrology* 105 (4): 369–80. doi:10.1007/BF00286825.

Cassar, N., J. P. Bellenger, R. B. Jackson, J. Karr, and B. A. Barnett. 2011. "N_2 Fixation Estimates in Real-Time by Cavity Ring-down Laser Absorption Spectroscopy." *Oecologia* 168 (2): 335–42. doi:10.1007/s00442-011-2105-y.

Cerling, T. E. 1984. "The Stable Isotopic Composition of Modern Soil Carbonate and Its Relationship to Climate." *Earth and Planetary Science Letters* 71 (2): 229–40. doi:10.1016/0012-821X(84)90089-X.

Cerling, T. E., and Jay Quade. 1993. "Stable Carbon and Oxygen Isotopes in Soil Carbonates." In *Climate Change in Continental Isotopic Records*, edited by P. K. Swart, K. C. Lohmann, J. Mckenzie, and S. Savin, 217–31. American Geophysical Union. http://onlinelibrary.wiley.com/doi/10.1029/GM078p0217/summary.

Chen, H., Winderlich, J., Gerbig, C., Hoefer, A., Rella, C. W., Crosson, E. R., Van Pelt, A. D., Steinbach, J., Kolle, O., Beck, V., Daube, B. C., Gottlieb, E. W., Chow, V. Y., Santoni, G. W. and Wofsy, S. C.: High-accuracy continuous airborne measurements of greenhouse gases (CO2 and CH4) using the cavity ring-down spectroscopy (CRDS) technique, Atmos Meas Tech, 3(2), 375–386, doi:10.5194/amt-3-375-2010, 2010.

Chiodini, G., S. Caliro, A. Aiuppa, R. Avino, D. Granieri, R. Moretti, and F. Parello. 2010. "First $^{13}C/^{12}C$ Isotopic Characterisation of Volcanic Plume CO_2." *Bulletin of Volcanology* 73 (5): 531–42. doi:10.1007/s00445-010-0423-2.

Chiodini, G., R. Coni, B. Raco and G. Scandiffio. 1991. Carbonyl sulphide (COS) in geothermal fluids: An example from Larderello field (Italy), *Geothermics 20 (5): 319-327.*

Conde, V., S. Bredemeyer, E. Duarte, J. F. Pacheco, S. Miranda, B. Galle, and T. H. Hansteen. 2013. "SO_2 Degassing from Turrialba Volcano Linked to Seismic Signatures during the

Period 2008–2012." *International Journal of Earth Sciences* 103 (7): 1983–98. doi:10.1007/s00531-013-0958-5.

Conde, V., P. Robidoux, G. Avard, B. Galle, A. Aiuppa, A. Muñoz, and G. Giudice. 2014. "Measurements of Volcanic SO_2 and CO_2 Fluxes by Combined DOAS, Multi-GAS and FTIR Observations: A Case Study from Turrialba and Telica Volcanoes." *International Journal of Earth Sciences* 103 (8): 2335–47. doi:10.1007/s00531-014-1040-7.

Crosson, E. R.: A cavity ring-down analyzer for measuring atmospheric levels of methane, carbon dioxide, and water vapor, Appl. Phys. B, 92(3), 403–408, doi:10.1007/s00340-008-3135-y, 2008Cerling, Thure E. 1984. "The Stable Isotopic Composition of Modern Soil Carbonate and Its Relationship to Climate." *Earth and Planetary Science Letters* 71 (2): 229–40. doi:10.1016/0012-821X(84)90089-X.

Emrich, K., D. H. Ehhalt, and J. C. Vogel. 1970. "Carbon Isotope Fractionation during the Precipitation of Calcium Carbonate." *Earth and Planetary Science Letters* 8 (5): 363–71. doi:10.1016/0012-821X(70)90109-3.

Fischer, T. P., C. Ramírez, R. A. Mora-Amador, D. R. Hilton, J. D. Barnes, Z. D. Sharp, M. Le Brun, et al. 2015. "Temporal Variations in Fumarole Gas Chemistry at Poás Volcano, Costa Rica." *Journal of Volcanology and Geothermal Research* 294 (March): 56–70. doi:10.1016/j.jvolgeores.2015.02.002.

Freundt, A., I. Grevemeyer, W. Rabbel, T. H. Hansteen, C. Hensen, H. Wehrmann, S. Kutterolf, R. Halama, and M. Frische. 2014. "Volatile (H_2O, CO_2, Cl, S) Budget of the Central American Subduction Zone." *International Journal of Earth Sciences* 103 (7): 2101–27. doi:10.1007/s00531-014-1001-1.

Gerlach, T. M., and B. E. Taylor. 1990. “Carbon Isotope Constraints on Degassing of Carbon Dioxide from Kilauea Volcano.” *Geochimica et Cosmochimica Acta* 54 (7): 2051–58. doi:10.1016/0016-7037(90)90270-U.

Gupta, P., Noone, D., Galewsky, J., Sweeney, C. and Vaughn, B. H.: Demonstration of high-precision continuous measurements of water vapor isotopologues in laboratory and remote field deployments using wavelength-scanned cavity ring-down spectroscopy (WS-CRDS) technology, Rapid Commun. Mass Spectrom., 23(16), 2534–2542, doi:10.1002/rcm.4100, 2009.

Hilton, D. R., C. J. Ramirez, R. Mora-Amador, T. P. Fischer, E. Furi, P. H. Barry, and A. M. Shaw. 2010. “Monitoring of Temporal and Spatial Variations in Fumarole Helium and Carbon Dioxide Characteristics at Poas and Turrialba Volcanoes, Costa Rica (2001-2009).” *Geochemical Journal* 44 (5): 431–40. doi:10.2343/geochemj.1.0085.

Javoy, M., F. Pineau, and H. Delorme. 1986. “Carbon and Nitrogen Isotopes in the Mantle.” *Chemical Geology* 57 (1–2): 41–62. doi:10.1016/0009-2541(86)90093-8.

Javoy, M., F. Pineau, and I. Iiyama. 1978. “Experimental Determination of the Isotopic Fractionation between Gaseous CO_2 and Carbon Dissolved in Tholeiitic Magma.” *Contributions to Mineralogy and Petrology* 67 (1): 35–39. doi:10.1007/BF00371631.

Keeling, C. D. 1958. “The Concentration and Isotopic Abundances of Atmospheric Carbon Dioxide in Rural Areas.” *Geochimica et Cosmochimica Acta* 13 (4): 322–34. doi:10.1016/0016-7037(58)90033-4.

Krevor, S., Perrin, J.-C., Esposito, A., Rella, C. and Benson, S.: Rapid detection and characterization of surface CO2 leakage through the real-time measurement of C

signatures in CO2 flux from the ground, Int. J. Greenh. Gas Control, 4(5), 811–815, doi:10.1016/j.ijggc.2010.05.002, 2010.

Lloyd, J, B Kruijt, DY Hollinger, J Grace, RJ Francey, SC Wong, FM Kelliher, et al. 1996. "Vegetation Effects on the Isotopic Composition of Atmospheric CO2 at Local and Regional Scales: Theoretical Aspects and a Comparison Between Rain Forest in Amazonia and a Boreal Forest in Siberia." *Functional Plant Biology* 23 (3): 371–99.

Lucic, G., J. Stix, B. Sherwood Lollar, G. Lacrampe-Couloume, A. Muñoz, and M. I. Carcache. 2014. "The Degassing Character of a Young Volcanic Center: Cerro Negro, Nicaragua." *Bulletin of Volcanology* 76 (9): 1–23. doi:10.1007/s00445-014-0850-6.

Lucic, G., Stix, J. and Wing, B.: Structural controls on the emission of magmatic cabon dioxide gas, Long Valley caldera, USA., in CCVG-IAVCEI 12th Field Workshop on Volcanic Gases, Northern Chile, 17 - 25 November., 2014.

Lucic, G., J. Stix, and B. Wing. 2015. "Structural Controls on the Emission of Magmatic Carbon Dioxide Gas, Long Valley Caldera, USA." *Journal of Geophysical Research: Solid Earth*, April, 2014JB011760. doi:10.1002/2014JB011760.

Malowany, K., Stix, J. and de Moor, J. M.: Field measurements of the isotopic composition of carbon dioxide in a volcanic plume and its applications for characterizing an active volcanic system, Turrialba volcano, Costa Rica., in CCVG-IAVCEI 12th Field Workshop on Volcanic Gases, Northern Chile, 17 - 25 November., 2014.

Malowany, K., J. Stix, and A. Van Pelt. 2015. "H_2S Interference on CO_2 Isotopic Measurements Using a Picarro G1101-I Cavity Ring-down Spectrometer." *Atmospheric Measurement Techniques Discussions* 8: 5651-5675. Doi:10.5194/amtd-8-5651-2015.

Martini, F., F. Tassi, O. Vaselli, R. Del Potro, M. Martinez, R. Van del Laat, and E. Fernandez. 2010. "Geophysical, Geochemical and Geodetical Signals of Reawakening at Turrialba Volcano (Costa Rica) after Almost 150 Years of Quiescence." *Journal of Volcanology and Geothermal Research* 198 (3–4): 416–32. doi:10.1016/j.jvolgeores.2010.09.021.

Mook, W. G., J. C. Bommerson, and W. H. Staverman. 1974. "Carbon Isotope Fractionation between Dissolved Bicarbonate and Gaseous Carbon Dioxide." *Earth and Planetary Science Letters* 22 (2): 169–76. doi:10.1016/0012-821X(74)90078-8.

Moussallam, Y., N. Peters, C. Ramírez, C. Oppenheimer, A. Aiuppa, and G. Giudice. 2014. "Characterisation of the Magmatic Signature in Gas Emissions from Turrialba Volcano, Costa Rica." *Solid Earth* 5 (2): 1341–50. doi:10.5194/se-5-1341-2014.

Munksgaard, N. C., Davies, K., Wurster, C. M., Bass, A. M. and Bird, M. I.: Field-based cavity ring-down spectrometry of δ13C in soil-respired CO2, Isotopes Environ. Health Stud., 49(2), 232–242, doi:10.1080/10256016.2013.750606, 2013.

Nara, H., H. Tanimoto, Y. Tohjima, H. Mukai, Y. Nojiri, K. Katsumata, and C. W. Rella. 2012. "Effect of Air Composition (N_2, O_2, Ar, and H_2O) on CO_2 and CH_4 Measurement by Wavelength-Scanned Cavity Ring-down Spectroscopy: Calibration and Measurement Strategy." *Atmosperic Measurement Techniques* 5 (11): 2689–2701. doi:10.5194/amt-5-2689-2012.

O'Keefe, A., and D. A. G. Deacon. 1988. "Cavity Ring-down Optical Spectrometer for Absorption Measurements Using Pulsed Laser Sources." *Review* of Scientific Instruments 59 (12): 2544–51. doi:10.1063/1.1139895.

OVSICORI, Observatorio Vulcanológio y Sismológico de Costa Rica. 2014. Boletin de Vulcanologia Estado de los Volcanes de Costa Rica, Octubre 2014.

Paonita, A., R. Favara, P. M. Nuccio, and F. Sortino. 2002. “Genesis of Fumarolic Emissions as Inferred by Isotope Mass Balances: CO_2 and Water at Vulcano Island, Italy.” *Geochimica et Cosmochimica Acta* 66 (5): 759–72. doi:10.1016/S0016-7037(01)00814-6.

Paonita, A., C. Federico, P. Bonfanti, G. Capasso, S. Inguaggiato, F. Italiano, P. Madonia, G. Pecoraino, and F. Sortino. 2013. “The Episodic and Abrupt Geochemical Changes at La Fossa Fumaroles (Vulcano Island, Italy) and Related Constraints on the Dynamics, Structure, and Compositions of the Magmatic System.” *Geochimica et Cosmochimica Acta* 120 (November): 158–78. doi:10.1016/j.gca.2013.06.015.

Pataki, D. E., J. R. Ehleringer, L. B. Flanagan, D. Yakir, D. R. Bowling, C. J. Still, N. Buchmann, J. O. Kaplan, and J. A. Berry. 2003. “The Application and Interpretation of Keeling Plots in Terrestrial Carbon Cycle Research.” *Global Biogeochemical Cycles* 17 (1): n/a – n/a. doi:10.1029/2001GB001850.

Protti, M., F. Gïendel, and K. McNally. 1995. “Correlation between the Age of the Subducting Cocos Plate and the Geometry of the Wadati-Benioff Zone under Nicaragua and Costa Rica.” *Geological Society of America Special Paper* 295 (January): 309–26. doi:10.1130/SPE295-p309.

Reagan, M., E. Duarte, G. J. Soto, and E. Fernández. 2006. “The Eruptive History of Turrialba Volcano, Costa Rica, and Potential Hazards from Future Eruptions.” *Geological Society of America Special Paper* 412: 235–57.

Rella, C. W., H. Chen, A. E. Andrews, A. Filges, C. Gerbig, J. Hatakka, A. Karion, et al. 2013. “High Accuracy Measurements of Dry Mole Fractions of Carbon Dioxide and Methane in Humid Air.” *Atmos. Meas. Tech.* 6 (3): 837–60. doi:10.5194/amt-6-837-2013.

Rizzo, A., H. Jost, A. Caracausi, A. Paonita, M. Liotta, and M. Martelli. 2014. “Real-Time Measurements of the Concentration and Isotope Composition of Atmospheric and Volcanic CO_2 at Mount Etna (Italy).” *Geophysical Research Letters* 41 (7): 2014GL059722. doi:10.1002/2014GL059722.

Sano, Y., and B. Marty. 1995. “Origin of Carbon in Fumarolic Gas from Island Arcs.” *Chemical Geology* 119 (1–4): 265–74. doi:10.1016/0009-2541(94)00097-R.

Sano, Y., and S. N. Williams. 1996. “Fluxes of Mantle and Subducted Carbon along Convergent Plate Boundaries.” *Geophysical Research Letters* 23 (20): 2749–52. doi:10.1029/96GL02260.

Shaw, A. M., D. R. Hilton, T. P. Fischer, J. A. Walker, and G. E. Alvarado. 2003. “Contrasting He–C Relationships in Nicaragua and Costa Rica: Insights into C Cycling through Subduction Zones.” *Earth and Planetary Science Letters* 214 (3–4): 499–513. doi:10.1016/S0012-821X(03)00401-1.

Snyder, G., R. Poreda, A. Hunt, and U. Fehn. 2001. “Regional Variations in Volatile Composition: Isotopic Evidence for Carbonate Recycling in the Central American Volcanic Arc.” *Geochemistry, Geophysics, Geosystems* 2 (10): 1057. doi:10.1029/2001GC000163.

Tassi, F., O. Vaselli, V. Barboza, E. Fernandez, and E. Duarte. 2004. “Fluid Geochemistry and Seismic Activityin the Period 1998-2002 at Turrialba Volcano (Costa Rica).” *Annals of Geophysics* 47 (4). doi:10.4401/ag-3355.

Taylor, B. E. 1986. “Magmatic Volatiles; Isotopic Variation of C, H, and S.” *Reviews in Mineralogy and Geochemistry* 16 (1): 185–225.

Taylor, J. R., and E. R. Cohen. 1998. "An introduction to error analysis: the study of uncertainties in physical measurements." *Measurement Science and Technology* 9.6: 1015.

Trolier, M., J. W. C. White, P. P. Tans, K. A. Masarie, and P. A. Gemery. 1996. "Monitoring the Isotopic Composition of Atmospheric CO2: Measurements from the NOAA Global Air Sampling Network." *Journal of Geophysical Research: Atmospheres* 101 (D20): 25897–916. doi:10.1029/96JD02363.

Vaselli, O., Franco Tassi, E. Duarte, E. Fernandez, R. J. Poreda, and A. Delgado Huertas. 2010. "Evolution of Fluid Geochemistry at the Turrialba Volcano (Costa Rica) from 1998 to 2008." *Bulletin of Volcanology* 72 (4): 397–410. doi:10.1007/s00445-009-0332-4.

Vogel, J. C., P. M. Grootes, and W. G. Mook. 1970. "Isotopic Fractionation between Gaseous and Dissolved Carbon Dioxide." *Zeitschrift Für Physik* 230 (3): 225–38. doi:10.1007/BF01394688.

Vogel, F. R., L. Huang, D. Ernst, L. Giroux, S. Racki, and D. E. J. Worthy. 2013. "Evaluation of a Cavity Ring-down Spectrometer for in Situ Observations of 13CO2." *Atmos. Meas. Tech.* 6 (2): 301–8. doi:10.5194/amt-6-301-2013.

Wallace, P. J. 2005. "Volatiles in Subduction Zone Magmas: Concentrations and Fluxes Based on Melt Inclusion and Volcanic Gas Data." *Journal of Volcanology and Geothermal Research*, Energy and Mass Fluxes in Volcanic Arcs, 140 (1–3): 217–40. doi:10.1016/j.jvolgeores.2004.07.023.

Watts, S. F.: The mass budgets of carbonyl sulfide, dimethyl sulfide, carbon disulfide and hydrogen sulfide, Atmos. Environ., 34(5), 761–779, doi:10.1016/S1352-2310(99)00342-8, 2000.

Zimmer, M. M., T.P. Fischer, D. R. Hilton, G. E. Alvarado, Z.. D. Sharp, and J. A. Walker. 2004. “Nitrogen Systematics and Gas Fluxes of Subduction Zones: Insights from Costa Rica Arc Volatiles.” *Geochemistry, Geophysics, Geosystems* 5 (5): Q05J11. doi:10.1029/2003GC000651.

Zobitz, J. M., J. P. Keener, H. Schnyder, and D. R. Bowling. 2006. “Sensitivity Analysis and Quantification of Uncertainty for Isotopic Mixing Relationships in Carbon Cycle Research.” *Agricultural and Forest Meteorology* 136 (1–2): 56–75. doi:10.1016/j.agrformet.2006.01.003.